Hydration Behavior of Polylactam Clathrate Hydrate Inhibitors and their Small-Molecule Model Compounds

*Andrea Perrin[a], Melissa J. Goodwin[a], Osama M. Musa[b], David J. Berry[c], Philip Corner[c], Katharina Edkins[c], Dmitry S. Yufit[a] and Jonathan W. Steed[a]**

a) *Durham University, Department of Chemistry, Lower Mountjoy, Stockton Road, Durham, DH1 3LE, UK, UK. Email: jon.steed@durham.ac.uk*

b) *Ashland Inc., 1005 Route 202/206, Bridgewater, NJ 08807, USA. E-mail: omusa@ashland.com*

c) *School of Medicine, Pharmacy and Health, Durham University, University Boulevard, Stockton-on-Tees, TS17 6BH, UK.*

KEYWORDS clathrate hydrate, kinetic hydrate inhibitor, lactam, pyrrolidone

Abstract

The solution hydration behavior of a series of lactam-based kinetic clathrate hydrate inhibitors (KHIs) has been studied in order to determine mechanistic insight into their KHI performance.

IR and ^{1}H NMR spectroscopic titration data were compared across a series of mono- and bis(lactam) model compounds, and solid-phase hydration behavior was examined by Dynamic Vapour Sorption. The structures of several of the model compounds have been investigated by X-ray crystallography. The work reveals insight into the very low crystallinity and high hygroscopicity of these materials which is linked to their performance as KHIs. Analysis of water binding in sour gas systems, containing H_2S and CO_2, reveals no effect on the water affinity of the lactams suggesting that sour gas components do not inhibit KHI performance, but rather promote clathrate hydrate formation.

Introduction

Clathrate hydrates are crystalline, non-stoichiometric host-guest compounds comprising a hydrogen bonded water framework entrapping small molecular guest species.[1-3] Methane hydrate in particular poses a major problem for the petrochemical industry with hydrate plug formation in under-sea pipelines causing safety concerns, and potentially costly pipeline shutdown.[4-6] The destructive nature of clathrate hydrates was highlighted in 2010 during efforts to contain the oil spillage following the Deepwater Horizon blowout.[7] Hydrate formation can be controlled using kinetic hydrate inhibitors (KHIs) such as polyvinyl pyrrolidinone (PVP) and polyvinylcaprolactam (PVCap).[8-10] PVCap in particular has proved to be highly efficient at delaying the onset of hydrate crystallization and is now industry-leading.[8] A range of copolymers based on PVCap have recently been reported[10] which impart additional useful properties such as high cloud point, biodegradability and corrosion resistance (Scheme 1). The presence of the vinylcaprolactam-derived component is apparently critical in these materials' ability to inhibit hydrate formation. However the KHI mode of action of this seven-membered-ring lactam is still

poorly understood. Broadly speaking there are three proposed mechanisms for the inhibition of clathrate hydrates,[10] namely:

(1) adsorption of the inhibitor onto the growing crystal surface;

(2) binding to a pre-critical hydrate nucleus preventing it from reaching critical size;

(3) structuring of water molecules in solution in order to prevent nucleation.

A plethora of techniques are used in order to gain insight into gas hydrate nucleation and growth, and the potential mode of action of KHIs on the macroscopic and microscopic scale.[11-13] There have been several recent developments in this area which are reliant on characterization of the resulting gas hydrate phases. In particular, high-pressure powder X-ray diffraction,[14] NMR spectroscopy and high-pressure calorimetry[15], have been used to probe inhibition using chemical KHIs or anti-freeze proteins.[13]

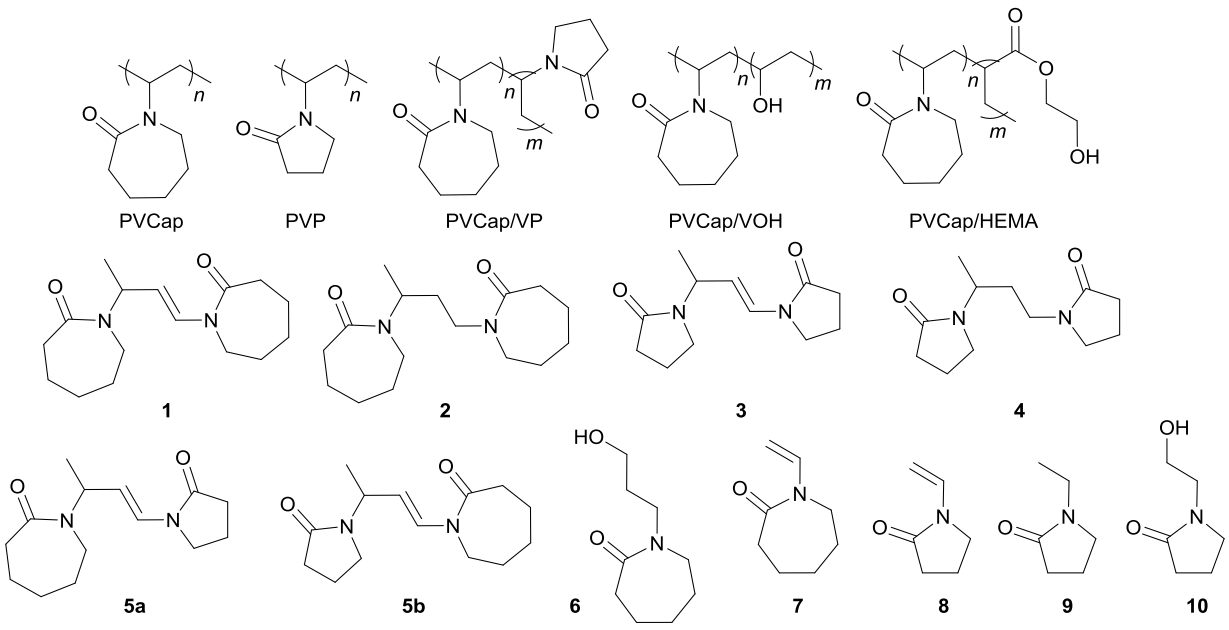

Scheme 1. Chemical structures of KHI polymers and their small-molecule model compounds.

It has been proposed that pendant functionalities on the KHI enable the adsorption of the inhibitor to the growing crystal surface, generally through hydrogen bonding to the lactam carbonyl functionality.[16] Following adsorption of the KHI, the hydrophobic backbone of the polymer restricts further hydrate growth, thereby reducing the likelihood of large scale hydrate formation and pipeline plugging.[16] Lee and coworkers have studied the adsorption of PVCap and PVP on cyclopentane hydrates.[17] While PVP follows a Langmuir isotherm, PVCap follows the BET-type; the combination of the increased molecular size and multilayer adsorption results in inhibition performance exceeding that for PVP.[17] Small-angle neutron scattering studies for poly(ethylene oxide), PVP, PVCap and a copolymer of VIMA/VCap on a model THF hydrate surface suggests that as the polymer adsorption to the surface increases, more growth sites are blocked.[18] By studying the THF hydrate system containing the respective inhibitor polymer both above and below the hydrate forming temperature, King *et al*. were able to observe conformational changes in the inhibitor polymers believed to be associated with the adsorption of the inhibitor to the hydrate surface.[18] Rodger and coworkers have incorporated an octamer sub-unit of PVP into the computational simulations of clathrate hydrate formation as an initial probe for KHI mechanism of action.[19] Their simulations indicate that PVP does not bind to the hydrate surface, but in fact stays approximately two solvation shells away from hydrate clusters.[19] They found that interaction between the polymer amide groups and water molecules effectively prevents nucleation. In addition, they found PVP to be ineffective at perturbing hydrate formation once clusters have reached a critical size.[19] Trout and coworkers have reported a simulation of KHI binding, proposing that the process of inhibition occurs via two steps:[20] (a) disruption of the organization of the water and guest molecules, increasing the barrier to nucleation, and (b) subsequent binding of the inhibitor to the growth face of the hydrate crystal,

thereby retarding the growth on the face on which the polymer is adsorbed.[20] The computational studies by Carver *et al*. into the adsorption behaviors of monomeric and oligomeric units with hydrate cages show that the strongest adsorption occurrs when each pyrrolidone oxygen atom forms two hydrogen bonding interactions with the hydrate surface.[21] Collectively these studies enable understanding, but have not elucidated a full story or the role of the lactam ring in hydrate formation and have not dealt with the question of hydrate formation in lower quality (sour) natural gas reserves.

We have previously reported preliminary results on water binding to model compounds **1** and **2** to gain insight into the nature of the interaction of water with lactam species before and during the early stages of hydrate crystallization. We now report detailed studies on a range of KHI polymers and model systems in order to address the role of the polymer in pre-nucleation water structuring. We also compare the water-binding data in 'sweet' systems with simulated 'sour gas' conditions in the presence of CO_2 and H_2S.[22] Sour gas fields have often been neglected because of the difficulty in removing the acid gas components. However, as natural gas reserves deplete they are of increasing interest.[22]

Results and Discussion

Polymer KHIs

Table 1. KHI polymers studied in the present work.

Name	Functionalities
PVP K12	Poly vinyl pyrrolidone, M_w = 3500

PVP K30	Poly vinyl pyrrolidone, M_w = 65,000
PVCap	Poly vinyl caprolactam, M_w = 3000
P(VCap/VOH)	Vinylcaprolactam-vinyl alcohol copolymer (82:18)
P(VCap/VP)	Vinylcaprolactam-vinyl pyrrolidone copolymer (95:5)
P(VCap/VP)	Vinylcaprolactam-vinyl pyrrolidone copolymer (50:50)
P(VCap/HEMA)	Vinylcaprolactam-(hydroxyethyl)methacrylate copolymer (95:5)

The interaction of water with a series of KHI polymers was examined by IR and ^{1}H NMR spectroscopic titration experiments. The composition of the polymers studied is described in Table 1. IR titrations with D_2O were carried out in acetonitrile which was selected as it is only a weak hydrogen bond donor and hence a poor competitor in hydrogen bonding to the lactam carbonyl functionality. D_2O is preferred over protic water because the OH bending mode of water overlaps the lactam carbonyl band of interest. Equivalents of the guest, D_2O, are calculated relative to the monomeric repeat unit in the lactam polymer.

The amide I carbonyl stretching frequency of PVP K12 occurs at 1668 cm^{-1} in the solid-state and at 1682 cm^{-1} in anhydrous acetonitrile (MeCN) solution. In comparison, for PVCap the C=O stretch occurs at 1629 cm^{-1} in the solid state and at 1637 cm^{-1} in anhydrous MeCN. Increased strain within the pyrrolidone ring reduces the contribution of the enolate resonance form, resulting in greater carbonyl double bond character than within the more flexible 7-membered caprolactam ring and hence the significantly higher carbonyl frequency in PVP. The differences between the solid-state and aprotic solution spectra for both polymers suggests stronger CH···O hydrogen bonding[23] in the solid-state leading to weaker C=O bonds.[24] Upon addition of up to

500 equivalents of D_2O, per monomer unit, in MeCN solution there is notable shift and broadening of the C=O stretch in both PVP and PVCap to 1658 cm^{-1} and 1616 cm^{-1} respectively (Figure 1). This observation is consistent with previous results which show that the frequency of the amide I band in a dry film of PVCap decreases on addition of up to 7 water molecules per monomer unit.[24-26] On a molar basis both polymers bind similarly to D_2O with cumulative υ(C=O) shifts for PVP and PVCap during the titration, totaling 24 cm^{-1} and 22 cm^{-1}, respectively. Comparison of PVP K12 with the high molecular weight PVP K30 revealed a similar overall carbonyl band shift and change in shape but the higher MW analogue saturates at a lower number of D_2O equivalents (See SI Figure S2). Work by Kelland and co-workers has shown that high MW PVP functions well by adsorbing to the hydrate surface, while low MW PVP has a greater effect upon gas hydrate nucleation.[27] The present work shows similar hydration behavior at the carbonyl moiety of both polymers in the solution.

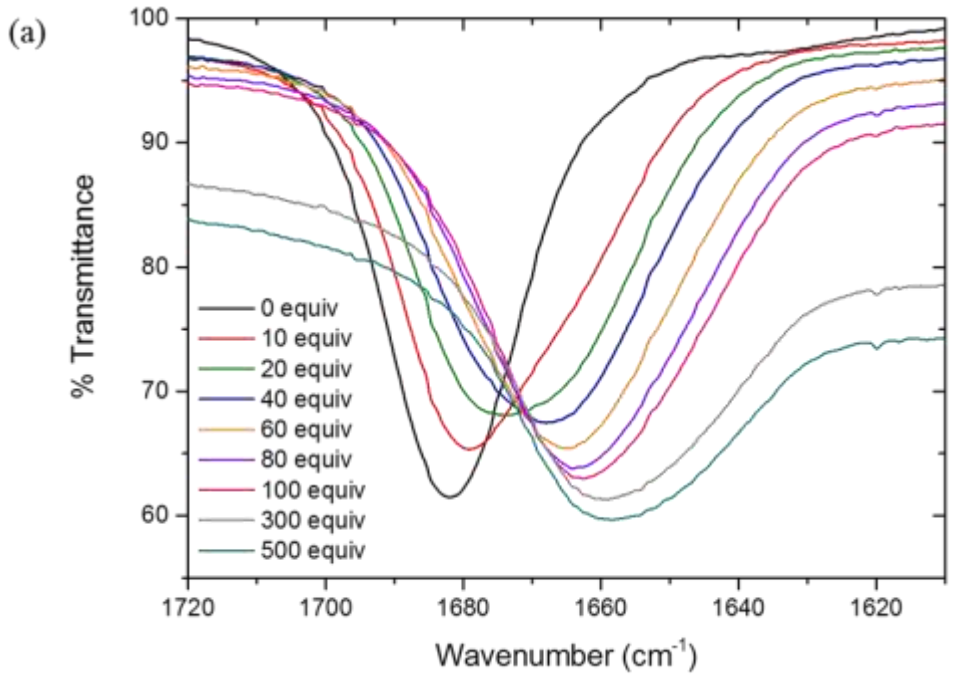

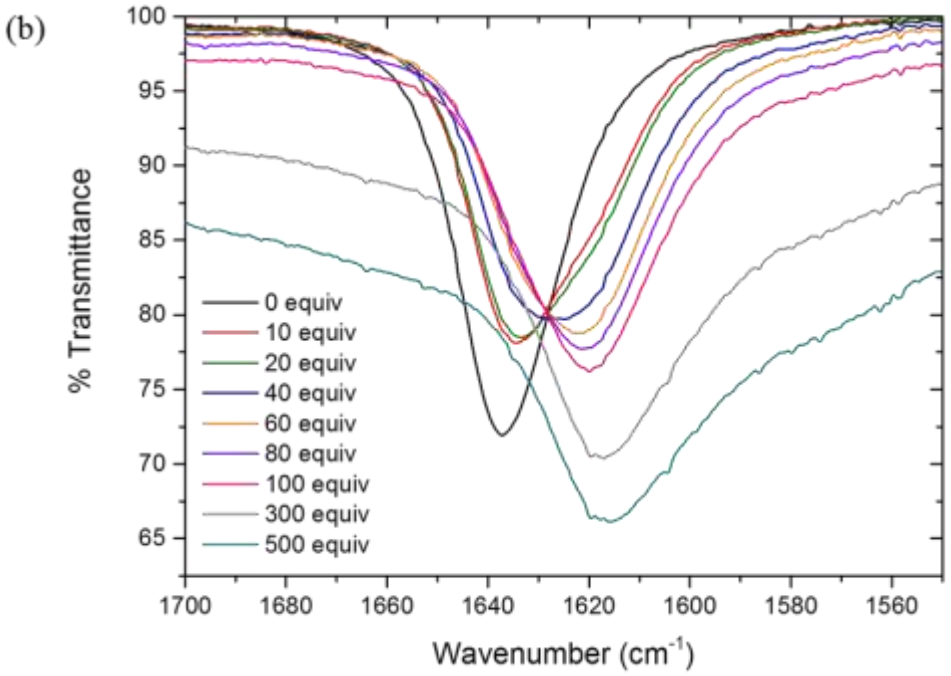

Figure 1. Solution IR titration results for (a) PVP K12 and (b) PVCap. Starting acetonitrile solutions were at a concentration of 5.38×10^{-5} mol/mL. D_2O molar equivalents are per monomer unit.

Broadening and asymmetry of the carbonyl bands during the titrations arises from the overlapping of multiple C=O bands as a result of multiple hydration states.[25] The resulting band asymmetry may be quantified according to the equation reported by Kirsh *et al.*[25] A significant change in the gradient of the plot of the band asymmetry as a function of added D_2O is attributed to the transition to a different hydrated carbonyl environment. Hence the band asymmetry may be used to monitor the evolution of the carbonyl stretch during hydration, and to enable systematic comparison between the polymer series. Broadened bands represent two (or more) different overlapping hydrated carbonyl bands.[26, 28-29] A broadened band is generally followed by a more symmetric band as more D_2O is added as a result of transition to the next hydrated state. Figure 2 shows the correlation between the titration data and the calculated carbonyl band

asymmetry for PVP K12 and PVCap. The behavior of PVP K30 is similar to PVP K12 (see SI Figure S4). The band asymmetry for both polymers shows a high dependence on the amount of D_2O added with up to four hydration states contributing to the spectrum, corresponding to the association of the lactam carbonyl with 0 – 3 molecules of D_2O as the deuterium oxide concentration increases. The gradient of the plots changes four times for both PVP and PVCap, suggesting the existence of up to four individual overlapping υ(C=O) bands. There is a significant difference between the PVP and PVCap in that that the more bulky PVCap appears to be more reluctant to bind higher numbers of water molecules, while its high polarity results in equally effective binding of the first equivalent.

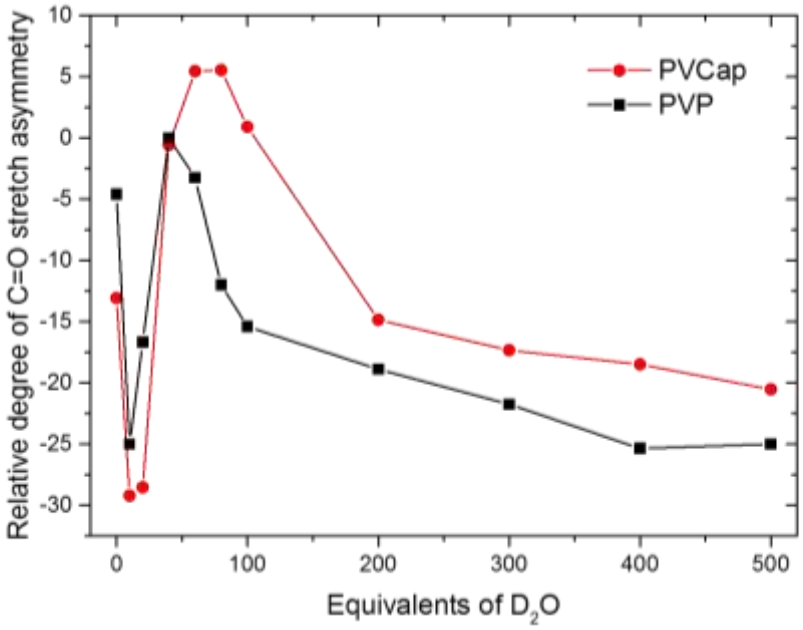

Figure 2. Relative degree of asymmetry of the C=O stretch in PVP and PVCap *vs.* molar equivalents of D_2O

The IR spectra of the lactam species were also recorded in pure D_2O to control for any dilution effects as a result of using MeCN solvent. This experiment gives the frequency of the amide I stretch for the fully hydrated species. The absence of dissociable protons within PVP and PVCap means that the IR bands should be approximately equivalent in H_2O and D_2O.[26] In 1, 5 and 10 wt% PVP-D_2O solutions the υ(C=O) occurs at 1645 cm^{-1} (see SI Figure S3) and remains unaffected by dilution. In addition, the absence of a carbonyl stretch at 1682 cm^{-1} confirms the lack of dehydrated carbonyl groups in aqueous solution. Hence the value of 1658 cm^{-1} seen in the titration with D_2O in MeCN represents significant but not complete hydration of the lactam functionality. Similarly, the υ(C=O) band occurs at 1609 cm^{-1} in a 1 wt% D_2O solution of PVCap, and at 1616 cm^{-1} in the PVCap-MeCN solution after addition of 500 equivalents of D_2O. The IR results for PVP and PVCap are summarised in Table 2.

Table 2. υ(C=O) for PVP K12 and PVCap in various states

	***v*(C=O) (cm^{-1})**				
Polymer	**Solid**	**MeCN**	**MeCN + 500 eqv. D_2O**	**MeCN + 1000 eqv. D_2O**	**1 wt% in D_2O**
PVP K12	1668	1682	1658	1653	1645
PVCap	1629	1637	1616	1614	1609

For further comparison PVP and PVCap were also titrated with 2-butoxyethanol in acetonitrile solution. Many KHIs are supplied commercially as 50 wt% mixtures in this alcohol. The most prominent carbonyl stretch at 1637 cm^{-1} in PVCap in MeCN solution remains largely unaffected by the addition of 2-butoxyethanol (Figure S5). Addition of more than 50 molar equivalents of 2-butoxyethanol results in a broad shoulder at ~1620 cm^{-1}, which increases in intensity as further solvent is added. We postulate that this shoulder corresponds to a butoxyethanol hydrogen-bonded species, the interaction is however clearly much weaker than with water and hence 2-butoxyethanol would not be expected to significantly influence KHI binding to water even though there is evidence that it acts as a 'synergist'.[30]

Two vinyl caprolactam-vinyl pyrrolidone copolymers with VCap:VP ratios of 50:50 and 95:5 were also examined. These copolymeric species exhibit high cloud points (72 ^{o}C for the 50:50 copolymer) and reasonable salt tolerance, making them appealing for warm field sites.[10] The hydration behavior of these compounds is of interest from the point of view of synergistic effects between the two lactam components and the fact that both functionalities can be monitored in the same experiment. Solution IR measurements clearly differentiate the pyrrolidone and caprolactam carbonyl bands in MeCN solution for the 50:50 copolymer, at 1680 cm^{-1} and 1635 cm^{-1}, respectively. Upon addition of 500 D_2O equivalents the υ(C=O) shifts to 1658 cm^{-1} for the pyrrolidone component and 1614 cm^{-1} for the caprolactam moiety, as shown in Figure 3.

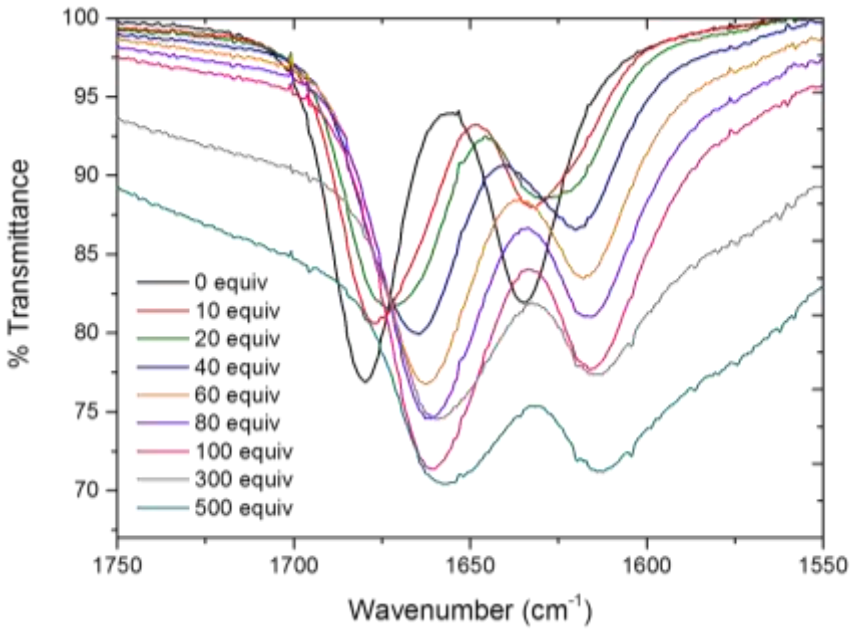

Figure 3. Solution IR titration showing addition of D_2O into an MeCN solution of the 50:50 VP/VCap copolymer. Starting solution concentration = 5.43×10^{-5} mol/mL.

The behavior of each component as a function of added D_2O closely mirrors that of the individual homopolymers and hence there does not appear to be any cooperative effect (Supplementary information Figure S6). In addition, changes in the relative degree of carbonyl band asymmetry highlight that the C=O band evolves in a similar manner in the 50:50 copolymer and respective homopolymers. The carbonyl region in the IR spectrum of the 95:5 VCap/VP copolymer is dominated by the caprolactam component, with the pyrrolidone stretch appearing as a broad shoulder throughout the titration. Prior to hydration the carbonyl stretches occur at 1676 cm^{-1} and 1636 cm^{-1} for the pyrrolidone and caprolactam groups respectively and the caprolactam band evolves similarly to the homopolymer upon titration with D_2O.

The hydration of the vinyl alcohol-vinyl caprolactam copolymer (VOH/VCap) was also studied. This species maintains KHI performance relative to PVCap, while having the additional

benefit of improved biodegradability.[10] The powdered KHI was isolated from its 2-butoxyethanol solvent through precipitation and repeated washing with diethyl ether and proved to be less soluble than PVCap in anhydrous MeCN. The solid-state IR spectrum shows a broad carbonyl stretch with a band maximum occurring at 1613 cm^{-1}, as seen in Figure 4b. This low ν(C=O) wavenumber represents a hydrogen-bonded species, akin to hydrated PVCap, however in this instance the shift to the enolate resonance form is believed to be as a result of intra-molecular hydrogen bonding interactions with the polymer OH functionalities. Such an interaction is expected to reduce the hydration potential of the polar C=O group. The carbonyl stretch is broad in the solid-state, indicating the presence of multiple carbonyl environments, but most notably contains a shoulder at higher wavenumber (approximately 1633 cm^{-1}) which is assigned to a "free" non-hydrogen bonded carbonyl stretching mode. In addition, a broad OH stretch occurs at 3500-3150 cm^{-1}, as expected for a hydrogen-bonded alcohol (Figure 4a).[16] Dissolution in MeCN, is likely to disrupt the intra-molecular interactions and expose a greater proportion of the carbonyl functionalities. The MeCN solution IR spectrum of the VOH/VCap copolymer has a broad carbonyl stretch at 1635 cm^{-1} with the shoulder occurring at lower wavenumber, as seen in Figure 4b. The OH stretch is shifted to higher wavenumber, and is split into two sharper peaks which are interpreted as arising from the presence of free OH groups on the polymer in addition to those intra-molecularly hydrogen-bonding to the C=O. The low solubility of the VCap/VOH copolymer in acetonitrile led to the use of a solution of lower concentration for titration with D_2O than in the analogous PVCap and PVP spectra and hence that data is noisier. A single carbonyl band is observed at 1609 cm^{-1} following addition of 500 equivalents of D_2O, similar to the fully hydrated VCap.

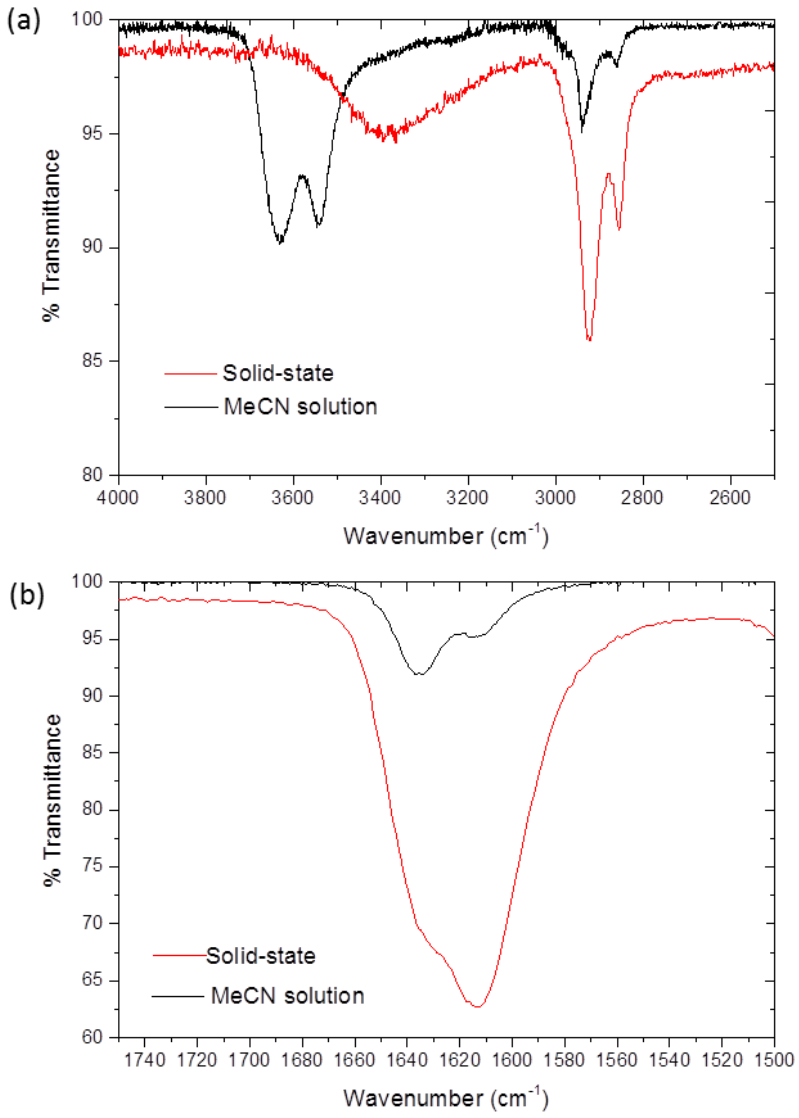

Figure 4. IR spectra of VCap/VOH copolymer in the solid-state and as an acetonitrile solution at a concentration of 3.28×10^{-5} moles/mL showing (a) ν(OH) and (b) ν(C=O)

Finally, we examined a biodegradable vinyl caprolactam–(hydroxyethyl) methacrylate (VCap/HEMA) copolymer (95:5).[31] Both the caprolactam C=O and HEMA C=O functionalities are apparent in the IR spectrum of an acetonitrile solution of this KHI, occurring at 1636 cm^{-1}

and 1720 cm^{-1} respectively (SI, Figure S10). The HEMA component is present in relatively small amounts within the copolymer, and as such is only observed as a broad shoulder of low intensity. During the titration the HEMA carbonyl stretch becomes too broad to accurately determine its position and asymmetry. The caprolactam carbonyl moiety behaves analogously to PVCap in terms of total wavenumber shift and asymmetry behavior. This suggests that the appended HEMA arm does not affect the hydration ability of the key caprolactam carbonyl group.

This work suggests that the superior KHI performance of PVCap in comparison to PVP does not arise from any superior ability to bind, or structure, liquid water. This work confirms that different functionalities can be incorporated upon the polymer backbone in order to address specific field-conditions without a significant effect upon the lactam carbonyl hydration. Even in the case of the intramolecularly hydrogen bonded VOH/VCap the interaction to the alcohol moiety is readily displaced by water binding.

Small Molecule Models

In order to obtain a more detailed understanding of the hydration behavior of oligolactam KHIs we turned to a number of small molecule model compounds designed to be simple enough to understand while retaining possible cooperative features arising from the presence of two adjacent lactam moieties as in the polymer systems. The unsaturated dimers **1** and **3** are readily obtained from the acid catalysed dimerization of VCap and VP, respectively. Subsequent hydrogenation gives bis(lactam) compounds **2** and **4**, which model PVCap and PVP, respectively (see experimental section). Compound **4** has been previously obtained from the acid catalysed dimerization of 1-vinyl-2-pyrrolidone (**8**) using trifluoroacetic acid in DCM.[32] However, in our hands the compound was more conveniently prepared as a viscous yellow oil by reaction of 1-vinyl-2-pyrrolidone with sulfuric acid in cyclohexane. We also prepared the mixed VCap/VP

dimer **5** as a mixture of isomers **5a** and **5b** which is of relevance as a model of the PVCap/VP copolymer. Reaction of a stoichiometric mixture of 1-vinyl-2-pyrrolidone and vinyl-caprolactam in cyclohexane with H_2SO_4 resulted in a viscous brown oil containing a mixture of homodimers **1** (caprolactam analogue) and **3** (pyrrolidone analogue) in addition to heterodimers **5a** and **5b**. The isomeric mixture of compounds **5** could be isolated by preparative HPLC and fractional crystallization resulted in a pure sample of **5a** that was analyzed by single crystal X-ray crystallography (*vide infra*). Unfortunately the challenge of purifying compounds **5** did not allow us to obtain sufficient material for binding studies. Compound **6** was prepared as a model for PVCap/VOH according to the procedure reported by Gracias *et al.*[33] and compounds **7** – **10** were also studied as comparative monomeric species.

Comparison of Model and KHI Hydration Behavior

In order to further understand the hydration of the lactam carbonyl group the hydration behavior of small-molecule model compounds **1** – **4** was studied using IR and ^{1}H NMR spectroscopy. Preliminary data on the hydration of caprolactam dimers **1** and **2** has been reported previously in a communication.[34] This work was repeated herein to ensure consistency across the series.

The IR spectrum of a dry acetonitrile solution of the unsaturated VP dimer **3** contains two carbonyl stretches, at 1701 cm^{-1} and 1680 cm^{-1}, as a result of the two distinct carbonyl functionalities. Unfortunately, the ν(C=C) band occurs at 1663 cm^{-1} in MeCN, and hence overlaps with the carbonyl stretches upon hydration (supplementary information Figure S14) it is therefore not possible to accurately trace the ν(C=O) shifts during the titration with D_2O.

IR spectroscopic measurements on saturated PVP analogue **4** as a neat film shows a ν(C=O) band at 1654 cm^{-1} which shifts to 1639 cm^{-1} as a 1wt% D_2O solution. These bands occur at lower wavenumber in comparison to PVP (1668 cm^{-1} and 1645 cm^{-1}) suggesting that the carbonyl groups are more accessible to both CH···O interactions in the solid state and OH···O interactions in water than PVP itself. However, the carbonyl stretch for **4** occurs at 1681 cm^{-1} in anhydrous MeCN solution, the same wavenumber as PVP K12, indicating that the apolar solvent successfully isolates the compound from intermolecular hydrogen bonding and hence **4** behaves analogously to the parent polymer. The model compound in dry acetonitrile was titrated with D_2O in the same way as the PVP polymers. The equivalents of D_2O are reported with respect to equivalents per lactam moiety in order to allow direct comparison between PVP and the model compounds. Hydration of the carbonyl moiety is observed by a shift from 1681 cm^{-1} to 1647 cm^{-1} upon addition of 500 molar equivalents of D_2O per lactam group, as seen in Figure 5. The greater accessibility of the carbonyl functionalities within the small dimer molecule may enable the binding of additional water, in contrast to the more sterically hindered polymer. This is highlighted by the greater cumulative wavenumber shift for **4** of 33 cm^{-1} compared to 24 cm^{-1} for PVP. The occurrence of asymmetric bands and several discrete maxima during the titration provide clear evidence that more than one hydrated species is formed.

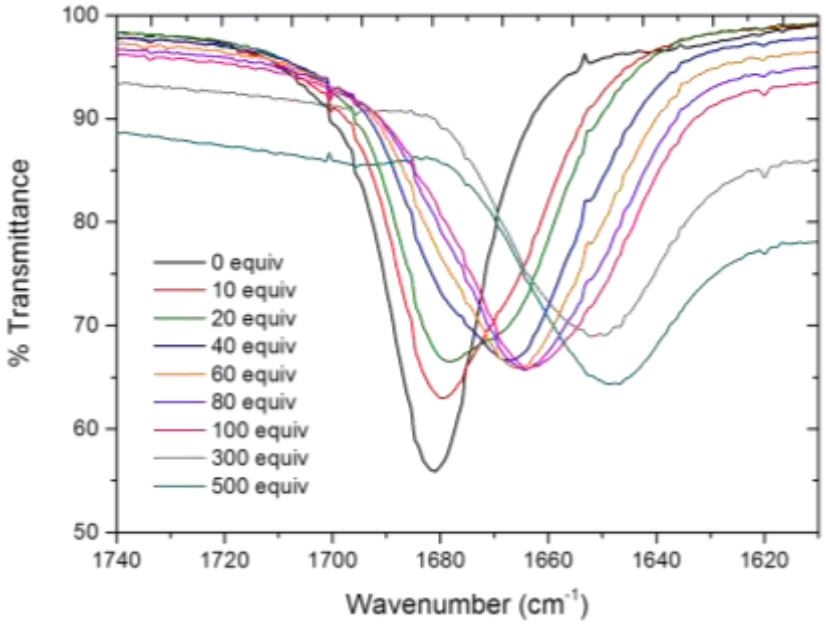

Figure 5. Solution IR spectroscopic titration showing addition of D_2O into an anhydrous MeCN solution of compound **4**. Equivalents of D_2O are calculated per lactam moiety.

Pyrrolidone monomers *N*-vinyl pyrrolidone (**8**) and *N*-ethyl pyrrolidone (**9**) have been used as models for PVP in computational simulations to provide insight into the mechanism of action of KHIs.[20-21] In order to examine the reliability of use of these monomeric lactam species as model compounds their solution behavior was investigated in comparison to bis(lactam) **4**. The *ν*(C=O) bands occur at 1704 cm^{-1} and 1681 cm^{-1} in anhydrous MeCN solutions of **8** and **9**, respectively. This indicates greater carbonyl double bond character in vinyl-pyrrolidone, which may be as a result of some delocalization of the nitrogen lone pair by conjugation with the alkene functionality.[35] Therefore, the saturated analogue **9** is expected to be more representative than **8** as a model for PVP. Figure 6 shows the IR titration data for the addition of D_2O to an acetonitrile solution of *N*-ethyl pyrrolidone (**9**).

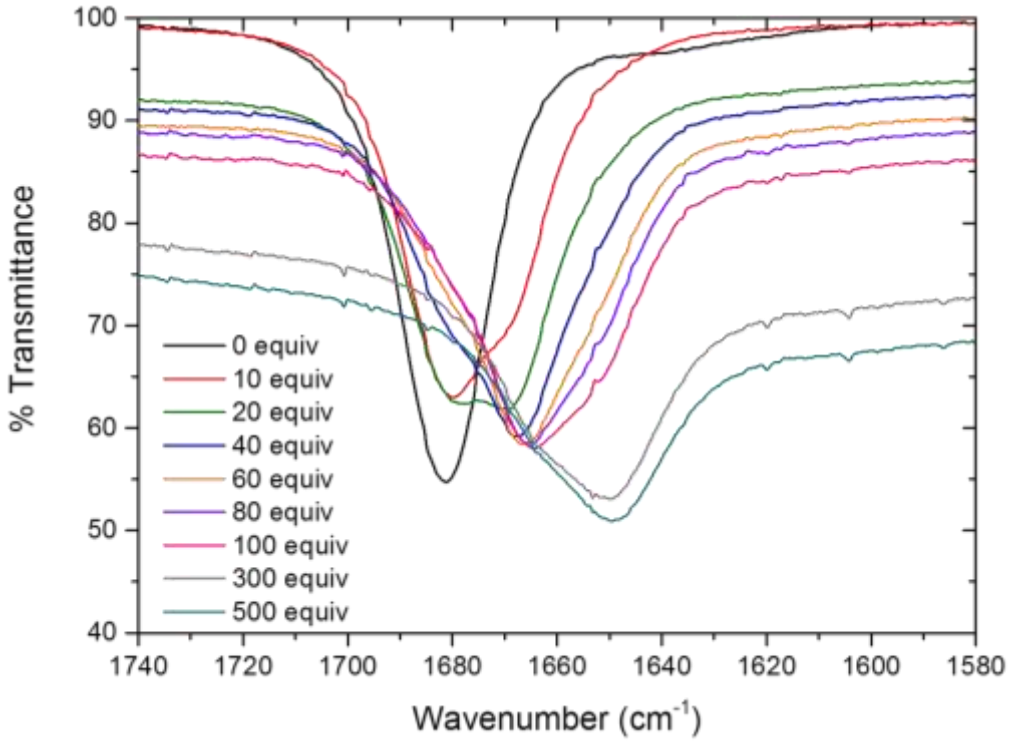

Figure 6. Solution IR titration showing addition of D_2O into an MeCN solution of ethyl pyrrolidone **9**. Starting solution concentration = 5.3×10^{-5} mol mL^{-1}.

Comparable changes in the relative degree of carbonyl stretching band asymmetry during titration validates the use of compound **4** as a model for PVP, as shown in Figure 7 alongside the data for saturated monomer **9**. The asymmetry trend for **4** upon addition of up to 100 D_2O equivalents closely mirrors that for PVP during the same initial hydration, with both plots showing three gradient changes. While the behavior of monomer **9** also shows three changes in gradient after addition of up to 100 D_2O equivalents, the second hydrated carbonyl stretch occurs at lower D_2O equivalents than for PVP and **4** (20 equivalents in **9** and at 40 equivalents for the dimer and polymer). The reduced steric hindrance in the monomer may make the carbonyl moiety more accessible to water, and therefore hydration could occur more readily. However, it is worth noting that further hydration (100 – 500 D_2O equivalents) results in an additional two

hydrated carbonyl environments for both the monomer and dimer, but only one further environment for PVP. Overall it appears that the dimeric compound is more suitable as a model for the hydration behavior of PVP, particularly when considering the first three hydrated environments. This may be rationalized in that the dimer is able to experience cooperative effects arising from adjacent carbonyl groups, which cannot occur in the monomeric model compound.

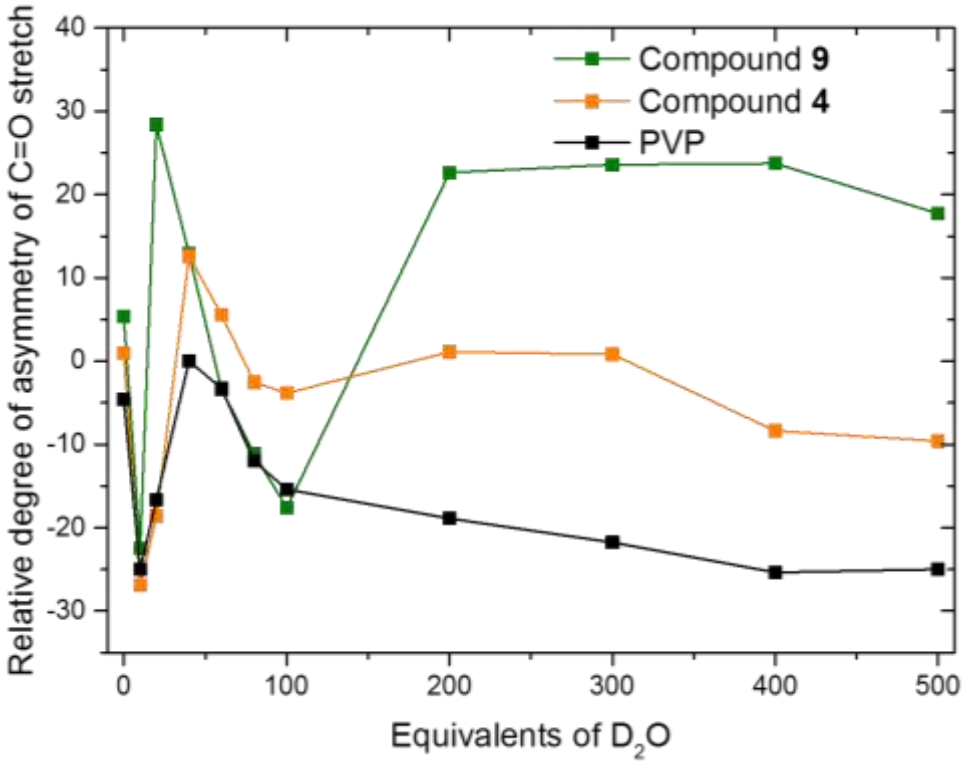

Figure 7. Comparison between the changes in the relative degree of carbonyl stretch asymmetry for PVP K12, **4** and **9**. Equivalents of D_2O are quoted per lactam unit.

Water binding by lactams **3**, **4**, **8** and **9** was also assessed by ^{1}H NMR spectroscopic titration.[36] Titrations were performed by adding D_2O to a solution of the isolated lactam in anhydrous acetonitrile-d_3. D_2O equivalents are quoted on a molar basis to facilitate calculations of binding

constants. Changes in chemical shift proved to be modest but reproducible, with the most significant changes noted for methylene protons on pyrrolidone rings with saturated substituents Figure 8, again confirming that ethyl-pyrrolidone and dimers such as **4** are better models for PVP hydration than vinyl-pyrrolidone.

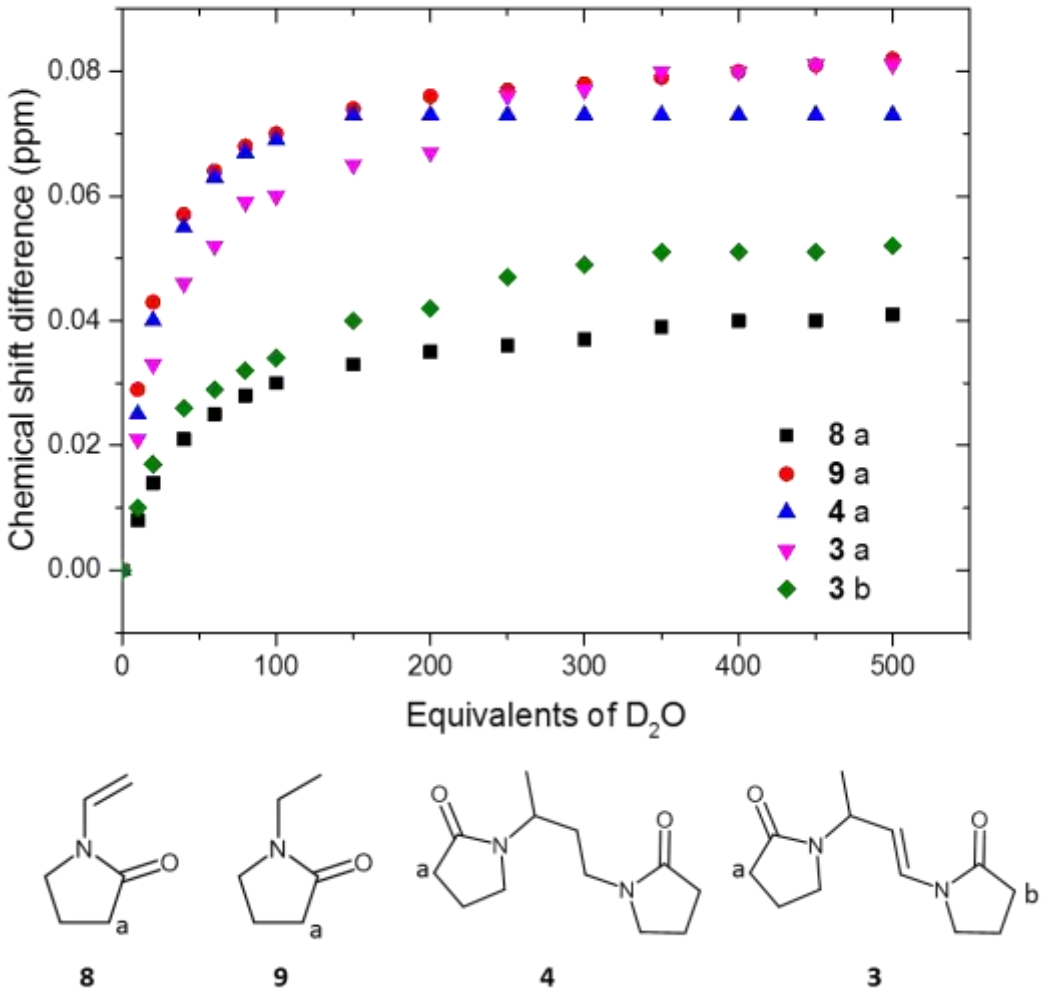

Figure 8. Chemical shift differences (ppm) for protons 'a' and 'b' adjacent to the carbonyl moiety in compounds **3**, **4**, **8** and **9**. Equivalents of D_2O are based on the entire lactam compound.

Equilibrium binding constants were calculated by non-linear least squares regression using HypNMR2006, and are given in Table 3.[37-38] In terms of the stoichiometry model the IR spectroscopic titrations have highlighted the occurrence of multiple guest binding, therefore a 1:1 stoichiometry is unlikely. However, given the weak binding it is not possible to unambiguously determine more than two equilibrium constants and hence a compromise 1:2 (H:G) stoichiometry model was adopted. In the case of bis(pyrrolidone) compounds **3** and **4**, the K_{11} binding constant corresponds to a single water molecule binding to one dimer molecule (possibly bridging between the two carbonyl groups), whilst K_{12} represents the binding of a second water molecule to give one water molecule per lactam carbonyl group. The titration isotherm for vinylpyrrolidone (**8**) fits a 1:1 stoichiometry, with a low binding constant of 0.05 M^{-1}, therein confirming its relatively poor hydration ability. The saturated monomer **9** shows a much greater propensity for hydration than **8**, as seen in the stronger binding constant of 0.62 M^{-1}. No significant difference was observed between the affinity of **9** and bis(pyrrolidone) **4** however, both experience a stronger interaction than the unsaturated **3**. The data for the bis(pyrrolidone) complex **4** is also very similar to bis(caprolactam) **2** confirming that both are suitable models but that water binding is sufficient weak that the experiment does not offer significant insight into the superior field performance of PVCap over PVP.

Table 3. D_2O Binding constants for model compounds by titration of up to 500 molar equivalents of D_2O into acetonitrile solutions of each compound.

Cpnd	**2**	**3**	**4**	**6**	**7**	**8**	**9**
Logβ_{11}	-0.29(4)	-0.37(2)	-0.22(6)	0.106(9)	-1.25(3)	-1.25(4)	-0.20(3)

K_{11}/M^{-1}	0.50	0.42	0.60	1.28	0.05	0.05	0.62
$\mathbf{Log}\beta_{12}$	-1.86(5)	-1.85(4)	-1.59(8)	-0.76(9)	-	-	-1.38(4)
K_{12}/M^{-1}	0.03	0.03	0.04	0.14	-	-	0.07

IR spectroscopic titration measurements were also undertaken for the caprolactam-vinyl alcohol **6**, a model for the PVCap/VOH copolymer. As a neat film compound **6** exhibits a broad carbonyl stretch occurs 1620 cm^{-1}. This is similar to the VCap/VOH copolymer (1613 cm^{-1}) itself, in which the broadness is thought to arise from multiple carbonyl environments due to varying intramolecular and/or intermolecular hydrogen bonding interactions. Upon dissolution in anhydrous acetonitrile, the broad carbonyl stretch in **6** resolves into two distinct bands, as shown in Figure 9. The band at higher wavenumber in MeCN solution (1637 cm^{-1}) is assigned to the "free" (*i.e.* non-hydrogen bonded) carbonyl groups, while that at lower wavenumber (1620 cm^{-1}) represents the carbonyl groups experiencing significant hydrogen bonding interactions from the OH functionalities in the molecule. It is not clear whether these are inter- or intramolecular interactions, although the X-ray crystal structure of 2-hydroxyethyl pyrrolidone (**10**) provides indirect evidence for intermolecular hydrogen bonding, (*vide infra*).

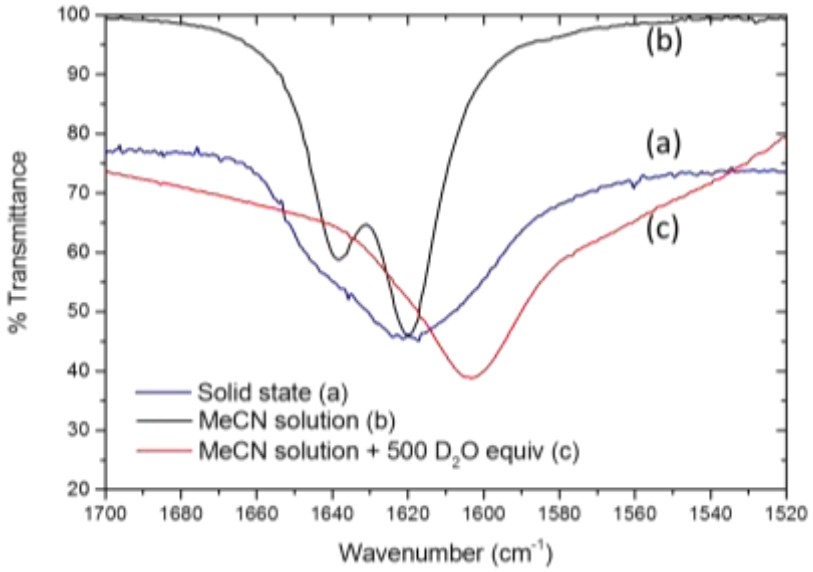

Figure 9. Partial IR spectra showing the carbonyl stretching band of compound **6** in (a) the solid state, (b) as an MeCN solution and (c) following addition of 500 D_2O equivalents to an MeCN solution.

Figure 10 compares the carbonyl stretch in acetonitrile solutions of the VCap/VOH copolymer and in model compound **6**. In both species the carbonyl stretch is resolved into two distinct bands of similar wavenumber. The band at higher wavenumber (1635 cm^{-1}) is dominant in the polymer, while the lower wavenumber band (1620 cm^{-1}) dominates in the model compound. This indicates that there is a greater degree of hydrogen-bonding interaction within the model compound than in the copolymer, likely as a result of the higher caprolactam:alcohol ratio in **6** (1:1 in **6** in comparison to 82:18 in the copolymer). Hence the hydration behavior of the caprolactam moiety of compound **6** may be an underestimate of that in the polymer.

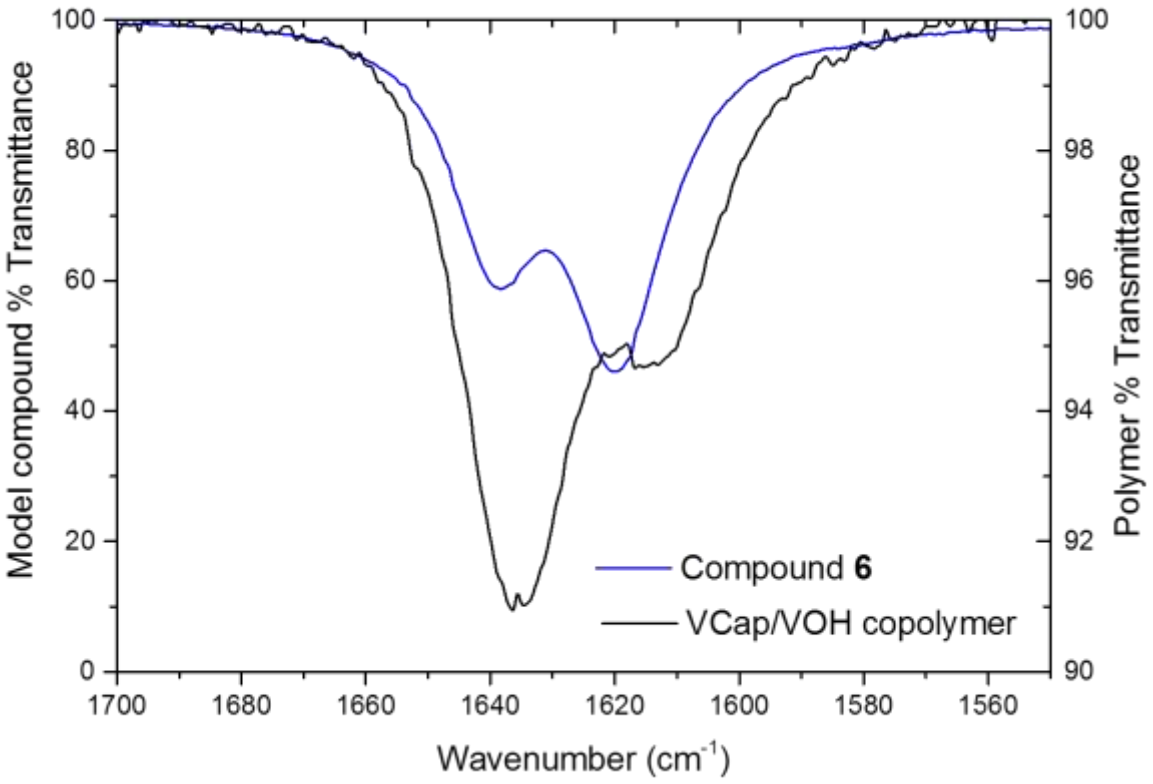

Figure 10. Comparison between the carbonyl stretch in MeCN solutions of (a) model compound **6** and (b) VCap/VOH copolymer.

The stepwise hydration of compound **6** was monitored through solution IR spectroscopic titration, as seen in Figure 11. Addition of only 10 D_2O molar equivalents results in a significant reduction in the intensity of the band at 1637 cm^{-1}, indicating transition to a hydrogen bonded carbonyl environment. Furthermore, the carbonyl stretch is then broadened at 40 D_2O equivalents, indicating transition to the next hydrated state. The carbonyl stretch occurs at 1603 cm^{-1} following addition of 500 D_2O equivalents; this is lower than the analogous band in the copolymer, indicating additional hydrogen bonding interactions in the smaller, more sterically accessible model compound. The hydration behavior of **6** is complex due to the two potential

hydration sites (C=O and OH), and the existence of two carbonyl bands in the MeCN solution, and as a result the band asymmetry information was not useful.

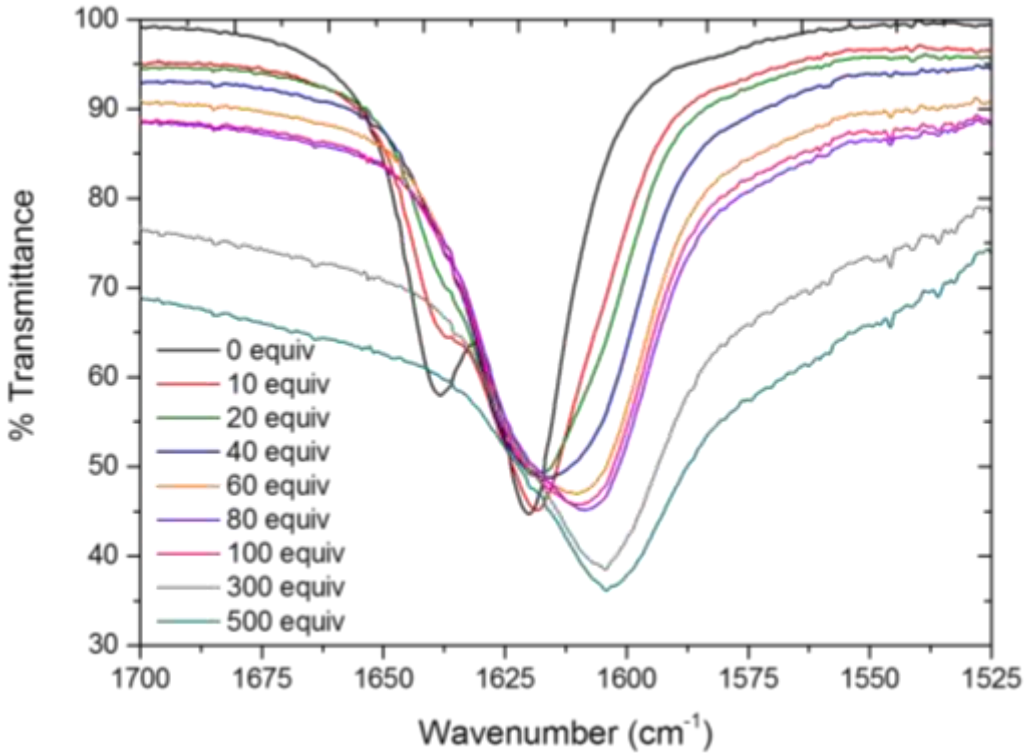

Figure 11. Solution IR titration showing addition of D_2O into an MeCN solution of compound **6**. Starting solution concentration = 5.84×10^{-5} mol mL^{-1}.

The ^1H NMR spectroscopic titration for compound **6** shows shifts in all protons (Supplementary information Figure S15). The alcohol OH proton occurs as a well-defined triplet at 3.74 ppm, and shifts downfield and broadens upon addition of D_2O as a result of hydrogen bonding interactions. It is possible to trace this resonance until addition of 250 D_2O equivalents, after which point the peak cannot be distinguished from the baseline because of exchange with deuterium. The resulting titration isotherm fits a combined 1:1 and 1:2 host:guest stoichiometry, with binding constants of 1.28 M^{-1} and 0.14 M^{-1} for K_{11} and K_{12}, respectively. These binding

constants are reasonably weak despite the presence of two potential water binding sites, albeit more significant than systems such as **2** and **4**.

For comparison, the hydration behavior of 2-hydroxyethyl pyrrolidone (**10**) was also studied. The carbonyl stretch in an acetonitrile solution of **10** is broadened (Supplementary information Figure S16), with a maximum at 1683 cm^{-1} in addition to a shoulder at lower wavenumber. In this species the most prominent carbonyl stretch, at higher wavenumber, represents the "free" carbonyl moieties. While the occurrence of intermolecular interactions has been established by the X-ray crystal structure (*vide infra*), the shortened aliphatic arm (in comparison to **6**) may reduce the potential for intramolecular interaction; hence the shoulder at lower wavenumber is of reduced intensity.

Finally, for completeness the solution behavior of *N*-vinyl caprolactam (**7**) was compared to the 5-membered analogue (**8**) in a further attempt to address the superior KHI performance of the caprolactam moiety. The titration isotherms for **7** and **8** both fit 1:1 host:guest stoichiometry. They both have low binding constants (Table 2), highlighting their poor hydration ability. In contrast the binding constants for compound **6** are much higher, confirming the improved hydration ability of saturated caprolactam compounds.

Sour Gas Systems

Natural gases, such as methane, are found mixed with acidic gases, particularly hydrogen sulfide and carbon dioxide. Above around 1 % H_2S content, the gas is classed as a sour gas.[22] Sour gas is often sweetened, in other words the acidic elements are removed, before being transported through pipelines since the presence of acidic gases causes corrosion, as well as promotes the formation of hydrates. H_2S forms clathrate hydrates at the lowest partial pressure of

all the components in sour gas, at least partially due to its size being correct to fit in the hydrate cavities.[39] The favorability of H_2S clathrate formation brings added hazards to the system, not least from the potential toxic effects of H_2S itself. The presence of H_2S changes the polarity of the system and increases the level of moisture in the gas.[40] The more water there is in the system, the higher the likelihood of it crystallizing and hydrates forming. In general, hydrates are more likely to form in sour systems than sweet ones in part due to the good fit of hydrogen sulfide in the clathrate hydrate cavity[41] as well as helping introduce water to form the hydrates. Considerable anecdotal evidence exists that clathrate hydrate formation is more severe in sour gas systems, which are being increasingly exploited commercially. To date there has been no research into the role of sour gas components on KHI mode of action. Insight into the interactions between sour gas and KHIs could lead to the development of more effect products for use in sour systems.

In order to address the effect of sour gas components on the interaction of KHIs and model compounds the IR and NMR titrations IR titrations of PVP, PVCap, VCap/VOH copolymer, and model compounds **1** – **4** were repeated in an identical fashion to the work described above in solutions saturated with CO_2 and with H_2S. The presence of the acid gases was confirmed by the characteristic IR signal for CO_2 at 2343 cm^{-1} and ^1H NMR resonance for H_2S at 1.07 ppm. Interestingly the results were identical within experimental error to the experiments in the sweet systems. Similarly NMR titration of model compound **4** withD_2O in the presence of CO_2 or H_2S did not show any difference to the analogous sour gas free experiment (see supplementary information for details).

These useful negative results imply that while acid gases, especially H_2S, have long been known to promote the formation of clathrate hydrates[5] there is no evidence in this study that they

materially affect the interaction of KHIs with water in a pre-nucleation situation. Hydrogen sulfide is commonly regarded as a clathrate hydrate 'help gas',[42-43] even allowing molecules which do not normal form clathrates to do so, and forms clathrates at the lowest pressure and highest temperature of any component in natural gas. The present work implies that the relative lack of efficacy of KHIs in sour gas fields would seem to be related to this facile formation of hydrates rather than any retardation of the inhibitor performance, at least as regards to pre-nucleation hydration behavior. Sour gases promote clathrate formation and hence more KHI is required to deal with the problem. This observation also explains why anti-agglomerants[8] are generally unaffected by gas composition.[41] Unlike KHIs, anti-agglomerants do not prevent the formations of clathrate hydrates but restrict particle size to give a free flowing slurry,[10] and hence faster or more prevalent clathrate formation does not greatly change their mode of action.

Water Vapor Sorption

In order to further assess the parallels between the model compounds and their parent polymers and in particular to assess the possibility of forming a crystalline hydrate phase for structural study, the water vapor sorption of bis(caprolactam) compounds **1** and **2** was assessed by Dynamic Vapor Sorption (DVS). Unsaturated compound **1** can be prepared in both amorphous and crystalline forms. Under ambient conditions it is a white crystalline powder. The amorphous form is stable and can be prepared by heating to 150 ^{o}C and then cooling the melt to room temperature. DVS analysis of crystalline and amorphous forms of **1** from 0 – 90 % relative humidity displayed very little weight gain (0.35 % and 1%, respectively) and essentially no hysteresis between sorption and desorption meaning that these unsaturated compounds are not particularly hygroscopic and do not form a crystalline hydrate phase. In comparison, solid PVCap itself displayed a weight gain of 16 % over the same humidity range (with around 1.8

water molecules per lactam group), implying significant hygroscopicity. This behavior is consistent with the known hygroscopicity of PVP. In our hands PVP K30 exhibited a weight gain corresponding to 2.5 water molecular per lactam group. No hysteresis was observed in these samples, implying no well-defined hydrated phase. In contrast, DVS analysis of the hydrogenated bis(caprolactam) **2** showed that, like the parent PVCap, this compound is also hydroscopic exhibiting a weight gain of 17.8% between 0 and 90% r.h., corresponding to 2.8 water molecules per molecule of **2** (around 1.5 water molecules per lactam; comparable to PVCap). The anhydrous sample did not begin to gain weight significantly until 60% r.h. and exhibited significant hysteresis on desorption implying the existence of a stable solid hydrate phase, Figure 12. Further increasing the humidity to 96% resulted in a 26.7% mass increase and hence very significant hygroscopicity.

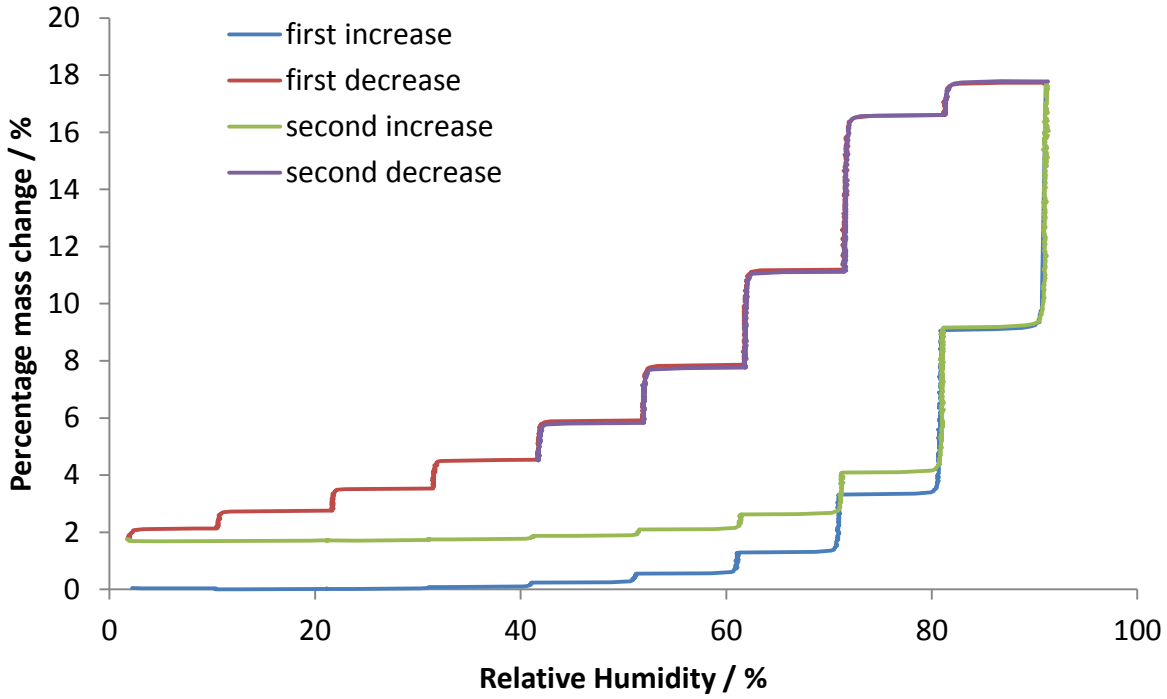

Figure 12. DVS analysis of model bis(caprolactam) **2**.

Model Compound Structural Analysis

The single crystal structures of several gas hydrates were reported in 2004.[44] We have previously reported the single crystal X-ray structures of compounds **1** and **2**,[2] which in the case of **1** show strong CH···O interactions between the C=O group and an alkene CH group. Extensive efforts were directed to the crystallization of hydrated forms of compounds **1** – **5** using conventional and *in situ* capillary crystallization techniques,[45] without success. The fact that single crystals of hydrated **2** were not isolated despite obtaining DVS evidence of their existence is disappointing and only samples of either ice or anhydrous **2** were obtained. The general difficulty in crystallizing this class of compound is, ironically, consistent with the fact that these materials are hydrate crystallization inhibitors.

Despite considerable efforts to crystallize the pyrrolidone based model compounds **3** and **4**, no crystalline material was obtained in conventional slow cooling and slow evaporation experiments. It is believed that the hygroscopicity of these species makes crystallization unlikely resulting in the substances occurring as oily residues in all instances. However, a sodium complex of metal-bound coordination complex of compound **4** has been previously reported[46] providing insight into the polarity of the pyrrolidone carbonyl moiety. It is of note that a diffraction quality crystal of the VP-based alkene **3** was obtained as large yellow needle shaped crystals by prolonged storing a sample of the compound at –20 ^{o}C in acetone under a CO_2 atmosphere as part of the sour gas experiments. The X-ray crystal structure is based on CH···O hydrogen bonding from the lactam ring methylene groups to the carbonyl oxygen atoms. The alkene CH groups are not involved in CH···O interactions but instead act as acceptors of weak CH···π hydrogen bonds. The crystal packing arrangement and Hirshfeld fingerprint analysis[47-48] is shown in Figure 13. The crystal density of 1.250 g cm^{-1} is relatively high compared to the

value of 1.231 g cm^{-1} for the caprolactam analogue (**1**) and markedly higher than the saturated compound **2** (1.162 g cm^{-1}), reflecting the less bulky nature of the pyrrolidone stopper groups. The two independent C=O bond lengths of 1.232(4) and 1.237(4) Å are identical within experiment error but the two amide C–N distances of N(1)–C(1) 1.344(3) and N(2)–C(8) 1.373(4) reflect some delocalization of the N(2) nitrogen lone pair across the alkene and hence less C=N double bond character in the N(2)-C(8) bond.

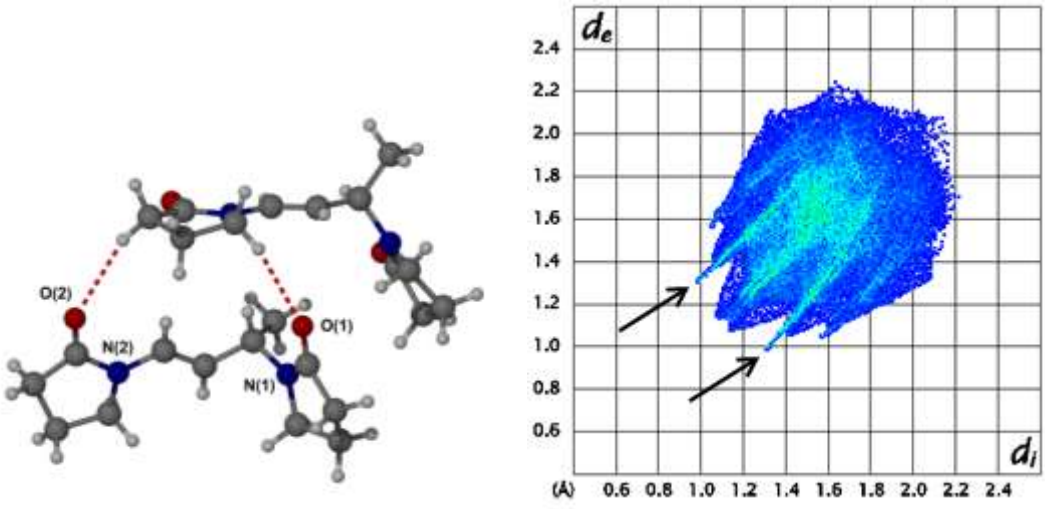

Figure 13. CH···O interactions in the crystal structure of **3** (b) Hirshfeld fingerprint analysis of **3** showing the prominent CH···O (arrows) and less prominent CH···C interactions.

It also proved possible to isolate diffraction quality crystals of heterodimer **5a** from an acetone/hexane mixture following slow evaporation of solvent. Due to the small crystal size, samples were analyzed at beam line I19 at the Diamond synchrotron, Oxfordshire, UK. The nitrogen-carbonyl bond distances are shorter than the N-C(ring) distances which is consistent with the partial double bond character for the N-C(O) bond upon transition to the enolate

resonance form. The caprolactam bond distance N(1)-C(1) of 1.365(2) Å is marginally shorter than the pyrrolidinone analogue N(2)-C(11) of 1.373(2) Å, although the difference is not statistically significant at the 3σ level. The two C=O distances are almost identical within experimental error.

The crystal packing in **5a**, shown in Figure 14, is based on CH···O interactions between the pyrrolidone carbonyl group and hydrogen atoms of a neighboring pyrrolidone (C···O distances of 3.461(3) Å and 3.490(3) Å), in addition to CH···O interactions between the caprolactam carbonyl functionality and the alkene group. The caprolactam carbonyl moiety is a better acceptor than the pyrrolidone analogue, and as such interacts with the stronger hydrogen bond donor of the alkene group rather than a methylene group. The caprolactam carbonyl-alkene interaction is marginally longer than that within the caprolactam homodimer (**1**), with distances of 3.390(3) Å and 3.320 Å for compounds **5a** and **1**, respectively.[34]

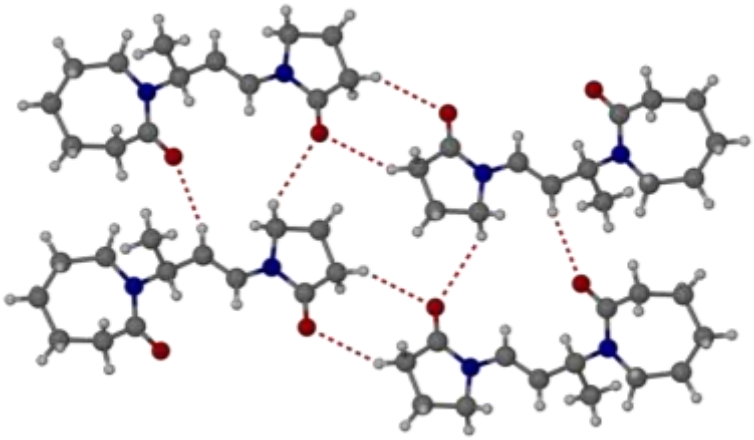

Figure 14. CH···O interactions in the crystal structure of **5a**.

The asymmetric nature of this compound results in less optimal packing than within unsaturated homodimer **1**, as exemplified by the densities of 1.207 g cm^{-3} and 1.231 g cm^{-3} for

5a and **1**[2] respectively (both at 120 K), hence **5a** is extremely poorly packed with a density comparable to the saturated homodimer **2** despite the better alkene CH···O hydrogen bond donors.[23] Hirshfeld surfaces[48-49] for **5a** and **1** (Figure 15) reveal that the CH···O interactions in **5a** are less pronounced than in **1** and instead **5a** exhibits significant CH···π interactions to the alkene double bond, absent in **1**. This suggests that the alkene is more accessible but overall the packing is less optimal.

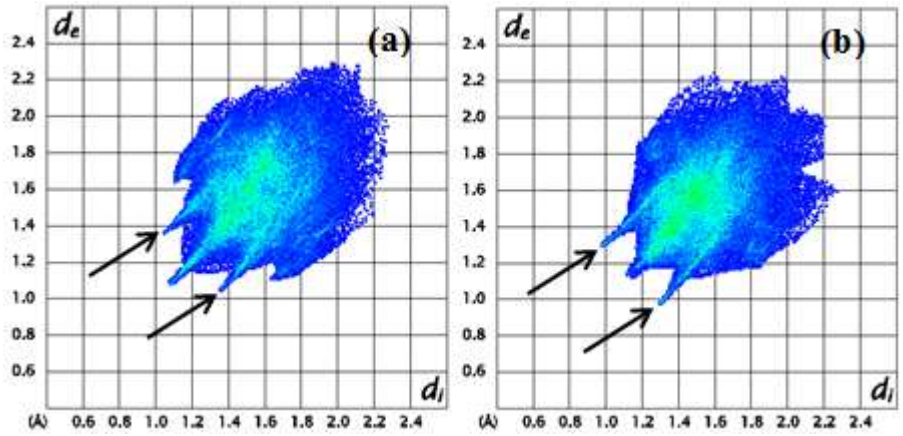

Figure 15. Hirshfeld surface fingerprint analysis for (a) **5a** and (b) **1**. Arrows highlight CH···O interactions. The two "wings" in (a) correspond to CH···π interactions.

For comparison the X-ray crystal structure of 1-vinyl-2-pyrrolidone (**8**) was also obtained and offers additional insight into pyrrolidone interactions in the solid-state. Compound **8** is a pale yellow liquid under ambient conditions (m.p. 13–14 ^{o}C[50]). *In situ* crystallization was performed by loading the liquid sample into a borosilicate glass capillary and subjecting the sample to a series of heating and cooling cycles to induce the formation of a single crystal (see Experimental section for details). Two datasets were collected, at 260 K and 150 K, and the material proved to be the same phase at both temperatures. In this compound the carbonyl oxygen atom forms a bifurcated acceptor CH···O hydrogen-bond to two hydrogen atoms of the alkene functionality,

with C···O distances of 3.3519(13) Å (C5-O1) and 3.3837(15) Å (C6-O1), as shown in Figure 16. In addition, there is a longer interaction between the carbonyl oxygen atom of one molecule with a lactam-CH_2 functionality. The Hirshfeld surface fingerprint plot is shown in Figure 18 alongside compounds **7** and **10** (*vide infra*).

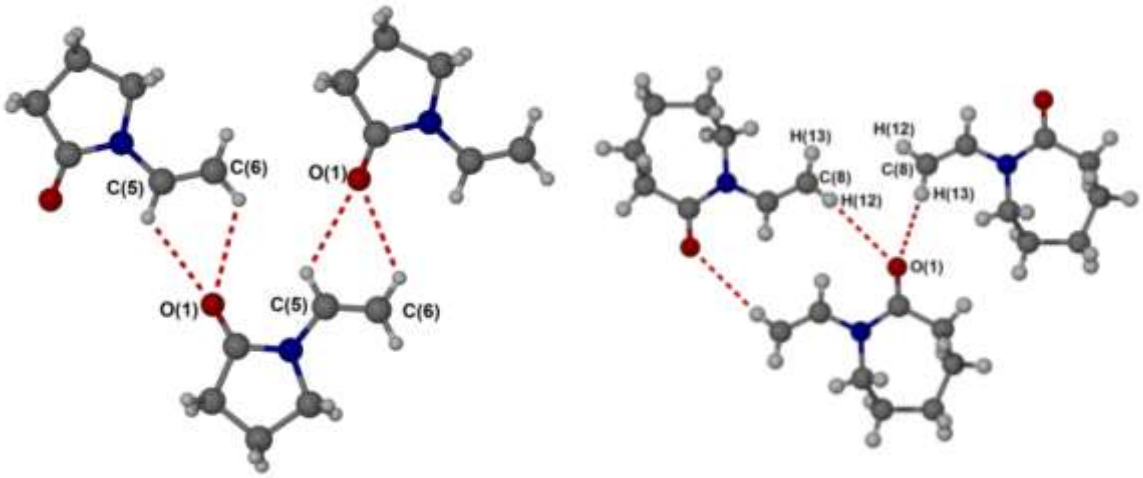

Figure 16. Crystal packing in (a) 1-vinyl-2-pyrrolidone (**8**) at 150 K and (b) *N*-vinyl caprolactam (**7**).[51]

Comparison between this unsaturated small lactam species with the 7-membered analogue is possible using the X-ray crystal structure of *N*-vinyl caprolactam (**7**) reported by Tishchenko *et al*. in 1997 (CSD refcode NUQYED).[51] The crystal packing differs from the pyrrolidone analogue, with a notable absence of a hydrogen bonding interaction between the caprolactam carbonyl moiety and the alkene-NCH proton, as seen in Figure 16b. The X-ray crystallographic analysis for **7** was conducted at room temperature and hence direct comparison on CH··O distances is not possible. We also examined 1-ethyl-2-pyrrolidone (**9**) as a comparator of **1**. Single crystals could not be obtained by *in situ* liquid crystallization, and repeated melt-freeze cycles resulted in the formation of a glass at low temperature. The lower melting point of -

77 ^{o}C for this compound, lack of a good hydrogen-bond donor, in addition to the flexibility and rotational freedom of the saturated ethyl arm may impede crystallization. Similarly attempts at *in situ* crystallization of a series of mixtures of **8**/**9** and of **9** with *N*-(2-hydroxyethyl)-2-pyrrolidone (**10**) also resulted only in glass formation.

It was also not possible to isolate single crystals of *N*-3-hydroxypropylcaprolactam **6** (the model compound for PVCap/VOH), but we anticipated that the solid-state structure of the more crystalline pyrrolidone hydroxyethyl analogue **10** may provide insight into potential intra- and intermolecular interactions in copolymers based on this type of repeat unit, particularly regarding the issue of intramolecular as opposed to intermolecular hydrogen bonding interactions, as noted in the IR studies of VCap/VOH. Flash cooling of **10** using a dry ice/acetone bath resulted in transformation of the yellow liquid to give a crystalline solid. The hygroscopic nature of this lactam is highlighted by the rapid transformation of this crystalline material to a liquid upon exposure to atmosphere. This process is apparently a result of the compound's deliquescence because when the crystalline material is held in a sealed environment, at room temperature, it remains solid indefinitely; however complete dissolution occurs within 15 minutes upon exposure to air. The X-ray crystal structure of **10**, collected at 120 K, demonstrates the presence of a short intermolecular hydrogen-bond between the hydroxyl donor and lactam carbonyl acceptor, with an O···O bond distance of 2.747(2) Å, Figure 17.

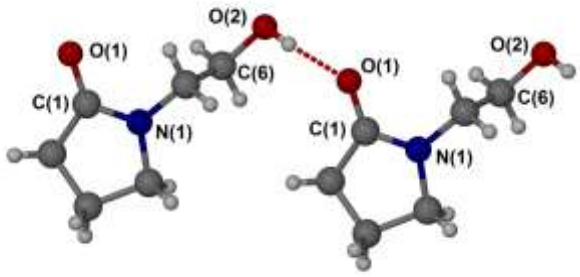

Figure 17. X-ray crystal structure of **10** showing the intermolecular hydrogen bonding interaction.

The Hirshfeld surface fingerprint plot for **10** is dominated by the intermolecular OH···O interaction (Figure 18c). Assuming that similar intermolecular interactions occur in the 7-membered analogue **6** and also in the VCap/VOH copolymer may explain the reduced solubility of the polymeric KHI. Intermolecular interactions would reduce the availability of the polar functionalities, and may lead to increased polymer aggregation with the polar groups inside the aggregate and an outward facing shell of greater hydrophobicity. In addition, such interactions would likely reduce the hydration potential of the species.

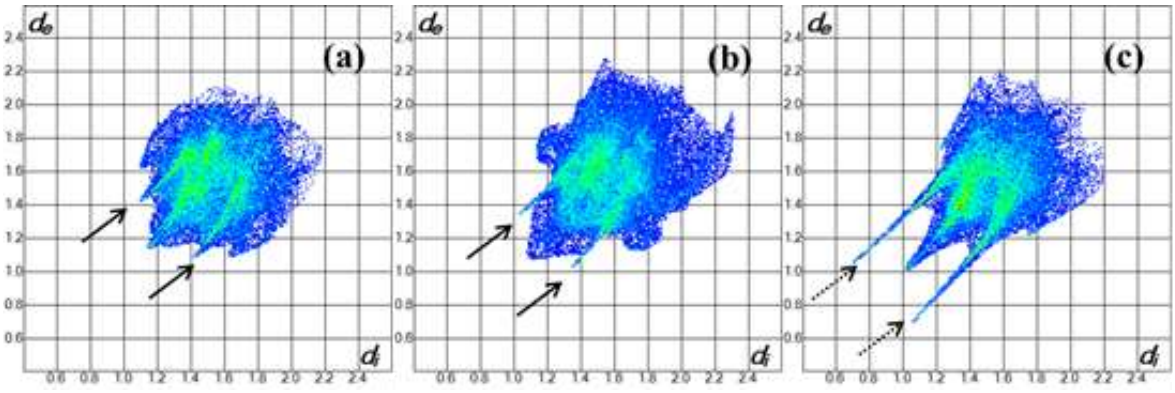

Figure 18. Hirshfeld surface fingerprint plots for (a) *N*-vinyl pyrrolidone **8**, (b) *N*-vinyl caprolactam **7** and (c) *N*-(2-hydroxyethyl)-2-pyrrolidone **10**. Solid black arrows on (a) and (b)

show CH···O interactions, dashed black arrow on (c) highlights the OH···O interactions. The two "wings" in (b) represent CH···π interactions.

Conclusions

IR spectroscopy has been utilized to gain insight into the hydrate inhibition behavior of a series of commercially available KHIs. All inhibitors undergo a step-wise hydration behavior with the lactam carbonyl group experiencing multiple hydrated environments. The carbonyl moiety appears to hydrate similarly amongst all of the compounds studied, irrespective of copolymer functionality. This is of relevance to the materials' industrial application since it implies that the KHI performance of the caprolactam groups in particular may not be significantly compromised by copolymeric functional groups designed to adapt performance to particular gasfield sites.

A selection of model compounds have been developed to represent the polymeric inhibitors in order to allow quantitative insight into water binding by this class of compound. At the molecular level the water binding by the polymeric species is closely mimicked by the saturated small molecule model compounds **2** and **4**. The presence of alkene groups significantly affects the hydration ability of monomeric *N*-vinyl caprolactam and vinyl-pyrrolidone, and suggests that use of saturated analogues of these monomers would provide a more realistic representation of the polymer hydration. The equilibrium water binding constants are very weak for all of the compounds studied; however, significant interactions to at least two water molecules per carbonyl group occurs in the presence of a large excess of water.

One postulate for the KHI mechanism of action suggests that inhibitors bind to water in solution, disrupt the formation of a structured cage and hence prevent the formation of clathrate

hydrates.[10] If this inhibition mechanism were to be the sole mode of functionality we would anticipate there to be a difference in the hydration behavior between PVCap and PVP given their different KHI performance. The absence of significant differences in the water binding properties of PVP and PVCap (and related model compounds) suggests that this KHI mechanism of action, if correct, is not the sole mechanistic explanation. However, to verify this theory further examination of the solution behavior should be conducted as a function of temperature and in the presence of the other pipeline components including NaCl and gas/oil molecules.

Despite DVS evidence for a hydrated form of **2**, the crystallization work reported herein demonstrates that this class of compound is extremely poorly crystalline as a result of the combination of good hydrogen bond acceptor but very poor hydrogen bond donor properties leading to a lack of self-complementarity and a significant propensity to absorb moisture. This behavior is likely to be linked to their clathrate hydrate inhibition behavior as well are the wide variety of uses of PVP in particular. It also suggests that this class of compound warrants further exploration in a crystallization inhibition context, for example in the stabilization of coamorphous phases.[52-53] The pure crystalline KHI analogues have low densities and are held together solely by weak interactions such as CH···O hydrogen bonding and CH···π interactions. Crystallization as hydrates or solvates is not observed presumably because of the presence of a significant hydrophobic backbone in the KHI analogues.

Experimental

Materials and Methods

Poly(lactam) KHIs were supplied by Ashland Inc. as 50 wt% mixtures in 2-butoxyethanol. The polymers were first isolated in powder form by precipitation with diethyl ether followed by

filtration. The samples were thoroughly dried, milled using a Retsch MM200 ball mill and dried using a vacuum drying pistol at 110 ^{o}C and the absence of residual solvent confirmed using ^{1}H NMR spectroscopy and IR spectroscopy. PVP samples were supplied as white powders and were analyzed after drying in the drying pistol. PVP K12 was purchased from Acros Organics and PVP K30 was supplied by Ashland Inc. 1-(2-hydroxyethyl)-2-pyrrolidone (**10**) was supplied by Ashland Inc. All other reagents and solvents were purchased from standard commercial sources and used without further purification. All NMR spectra were performed on a Varian Mercury-400 MHz (^{1}H, ^{13}C) and Bruker Advance-400MHz (^{1}H, ^{13}C) and were referenced to residual solvent. Electrospray (ES) mass spectrometry was recorded on a Thermo-Finnigan LTQ instrument.

HPLC was performed using a Waters Mass Directed Auto-Purification system equipped with an XBridge Prep C18 column (100 x 19 mm, 5um) with a linear gradient elution from 90% water with 0.1% formic acid and 10% acetonitrile with 0.1% formic acid to 5% water with 0.1% formic acid and 95% acetonitrile with 0.1% formic acid over 10 minutes.

Crystals suitable for single crystal X-ray diffraction structure determination were immersed in perfluoropolyether oil and mounted on a preformed tip. Single crystal X-ray data for compounds **8**, **10** and the precursor to 6 (see supplementary information) were collected on an Agilent XCalibur diffractometer (Sapphire-3 CCD detector, fine-focus sealed tube, graphite monochromator, MoKα-radiation, λ = 0.71073 Å) and for compound **3** on a Bruker D8Venture (Photon100 CMOS detector, IμS-microsource, focusing mirrors, CuKα-radiation, λ = 1.54178 Å). The data for the structure of **5a** were collected on a Rigaku Saturn 724+ diffractometer at station I19 of the Diamond Light Source synchrotron (undulator, λ = 0.6889 Å, ω-scan, 1.0°/frame) The temperature on the samples was maintained by Cryostream (Oxford

Cryosystems) open-flow nitrogen cryostats. All structures were solved using direct methods and refined by full-matrix least squares on F^2 for all data using SHELXL[54] and OLEX2[55] or X-Seed.[56] All non-hydrogen atoms were refined with anisotropic displacement parameters. CH hydrogen atoms were placed in calculated positions, assigned an isotropic displacement factor that is a multiple of the parent carbon atom and allowed to ride. H-atoms attached to oxygen were located on the difference map when possible, or placed in calculated positions. Crystal data and parameters of refinement are listed in the relevant experimental sections. Crystallographic data for the structures have been deposited with the Cambridge Crystallographic Data Centre as supplementary publications CCDC 1525989-1525993.

IR Spectroscopic measurements

Fourier transform infrared spectra were recorded using a Perkin Elmer Spectrum 100 μATR spectrometer. For each solid-state spectrum, 16 scans were conducted over a spectral range 4000 to 600 cm^{-1} with a resolution of 1 cm^{-1}. For solution measurements a Specac solution IR cell was used, which was fitted with CaF_2 windows using a 0.05 mm spacer. The analysis was carried out using the Perkin Elmer Spectrum Express 1.01 software. Solution IR spectroscopic titrations with D_2O were performed by dissolving the dry KHI polymer powder in anhydrous acetonitrile (MeCN) to generate a homogeneous solution of known concentration.

General procedure for ^{1}H NMR spectroscopic titrations

All chemical shifts are reported in ppm relative to residual solvent. A solution of the host species of known concentration was made up in a single NMR tube using d_3-acetonitrile. D_2O was added in 10 μL aliquots using a Hamilton microliter syringe and the spectra were recorded after addition. Analysis was performed using HypNMR2006[38] with choice of stoichiometric

model informed by the IR titration data and dictated by the best fit to the titration data. Titration isotherms are included in the Supplementary Material.

Synthesis

*1,3-Bis(caprolactam-2-on-1-yl) but-1-ene (**1**)*

N-vinyl caprolactam (2.0 g, 14.4 mmol) and dry hexane (10 mL) were placed into a 3-neck round bottom flask fitted with a stirrer bar, reflux condenser and nitrogen inlet/outlet. The reaction mixture was heated to 50 ^{o}C and TFA (4 drops) was added through the sidearm. The temperature was increased to 60 ^{o}C and held for 3 h. The mixture was allowed to cool to room temperature, under nitrogen, whereby two layers were visible. Hexane (40 mL) was added and a white precipitate formed. The solid product was isolated using Büchner filtration. The product was washed with cold hexane if residual *n*-vinyl caprolactam remained. The ^{1}H NMR spectrum was in agreement with published work.[34]

*1,3-Bis(pyrrolidin-2-on-1-yl) but-1-ene (**3**)*

N-vinyl pyrrolidone (12 g, 108 mmol) was placed into a 2-neck flask under an atmosphere of nitrogen, and anhydrous cyclohexane (5 mL) was added. The reaction mixture was heated to 60 ^{o}C with stirring. Concentrated sulphuric acid (3 μL) was added and the temperature was increased to 70 ^{o}C. The reaction mixture was held at 70 ^{o}C, under nitrogen, for 6 h. The mixture was then allowed to cool to room temperature, and the solvent removed upon the rotary

evaporator. Residual solvent and acid were removed by addition of hexane (20 mL) followed by rotary evaporation. Prior to analysis, the sample was held in the drying pistol at 110 ^{o}C for 3 h. ^{1}H NMR (400 MHz, $CDCl_3$) δ 6.98 (d, *J* = 13.6 Hz, 1H, NCH), 4.95 – 4.83 (m, 2H, CH=CH), 3.49 – 3.43 (m, 2H, NCH_2), 3.31 – 3.23 (m, 2H, NCH_2), 2.47 (t, *J* = 8.2 Hz, $COCH_2$), 2.40 – 2.33 (m, 2H, $COCH_2$), 2.10 (d, *J* = 7.4 Hz, 2H, CH_2), 2.01 – 1.93 (m, 2H, CH_2), 1.27 (d, *J* = 6.8 Hz, 3H, CH_3). ^{13}C{^{1}H} NMR (100 MHz, $CDCl_3$) δ 174.36, 173.42, 125.26, 110.89, 46.15, 45.35, 42.55, 31.65, 31.34, 18.11, 17.58, 17.11. IR (*v*/cm^{-1}): 1674 (C=O), 1658 (C=O). Crystal data: $C_{12}H_{18}N_2O_2$, space group *Pca*2$_1$, *a* = 12.4684(9) Å, *b* = 10.6073(8) Å, *c* = 8.9326(6) Å, *V* = 1181.39(15) Å^3, Z = 4, D_c = 1.250 g/cm^3, *F(000)* = 480.0, CuKα (λ = 1.54178) 2θ range for data collection = 8.34 – 139.88°, data = 2074, parameters = 146, goodness-of-fit on F^2 = 1.084, R_1 = 0.0583, wR_2 = 0.1860

*1-caprolactamyl,3-(2-pyrrolidone-1-yl) but-1-ene (**5a**)*

N-vinyl caprolactam (2.0 g, 14.4 mmol) and *n*-vinyl pyrrolidone (1.6g, 14.4 mmol) were added to a 3-neck round bottom flask fitted with a stirrer bar, reflux condenser and nitrogen inlet and outlet. Trifluoroacetic acid (8 drops) was added through the sidearm, and the reaction mixture was stirred at room temperature for 3 hours, under N_2, resulting in a viscous yellow oil. Dry hexane (10 mL) was added, and the reaction mixture was heated to 50 ^{o}C and held for 19 hours. Upon cooling to room temperature, the hexane layer was decanted to isolate a thick yellow/orange oil. Silica column chromatography using an acetone/hexane (3:1) solvent system results in the isolation of compound **5** as a mixture of isomers **5a** and **5b**. Single crystals of **5a** are isolated by slow evaporation from methanol. ^{1}H NMR (400 MHz, $CDCl_3$) *δ* 6.96 (dd, *J* = 1.7,

14.8 Hz, 1H, vinyl NCH), 5.40 (m, J = 3.4, 5.9, 10.1 Hz, 1H, NCH), 4.90 (dd, J = 5.0, 14.8 Hz, 1H, vinyl CH), 3.50-3.43 (m, 2H, CH_2), 3.19 – 3.11 (m, 2H, CH_2), 2.55 – 2.44 (m, 4H, 2 x CH_2), 2.09 (m, J = 7.6, 14.8 Hz, 2H, CH_2), 1.68 – 1.66 (m, 6H), 1.22 (d, J = 6.9 Hz, 3H, CH_3). $^{13}C\{^1H\}$ NMR (100 MHz, $CDCl_3$) δ 175.74, 173.58, 125.44, 112.32, 48.46, 45.58, 43.49, 37.91, 31.55, 30.34, 30.05, 23.79, 17.73, 16.99. MS (GC ES-) *m/z*: 249.1 (M-H). IR (cm^{-1}): 1622 (C=C), 1658 (C=O) and 1690 (C=O). Crystal data for $C_{14}H_{22}N_2O_2$, M = 250.34, colorless block, 0.30 x 0.10 x 0.05 mm^3, triclinic, space group $P\bar{1}$ (no. 2), a = 6.353(3) Å, b = 8.231(4) Å, c = 14.087(10) Å, α = 102.473(8)°, β = 96.293(8)°, γ = 103.742(5)°, V = 688.5(7) $Å^3$, Z = 2, D_c = 1.207 g/cm^3, F_{000} = 272, λ = 0.68890 Å, T = 120(2)K, $2\theta_{max}$ = 52.0°, 6733 reflections collected, 2785 unique (R_{int} = 0.0335). Final *GooF* = 1.076, *R1* = 0.0605, *wR2* = 0.1667, *R* indices based on 2411 reflections with I>2σ(I) (refinement on F^2), 164 parameters, 0 restraints.

*Hexahydro-1-(3'-hydroxypropyl)-2H-azepin-2-one (**6**)*

Compound **6** was prepared according to the procedure reported by Gracias *et al.*[33] 3-Azido-1-propanol[57] (0.5 g, 4.94 mmol) - **CARE small molecule azides can be potentially explosive** - was added to a solution of cyclohexanone (0.485 g, 4.94 mmol) in dry DCM (12 mL) under N_2. The mixture was stirred and cooled to 0 °C. $BF_3.OEt_2$ (1.22 mL, 9.89 mmol) was added dropwise over 5 minutes, noting some gas evolution. The solution was warmed to room temperature over 30 minutes, and then stirred at room temperature for an additional 3 hours. The solution was concentrated, saturated $NaHCO_3$ (20 mL) added and the mixture stirred at room temperature for 60 minutes. DCM (80 mL) was added then the organic layer was separated, dried (using $MgSO_4$) and concentrated to a viscous oil. Silica column chromatography, with an ethyl acetate eluent,

enables clean isolation of the product as a yellow oil (0.603 g, 3.52 mmol, 71 %). ^{1}H NMR (400 MHz, CD_3CN) δ 3.74 (t, 1H, OH), 3.44 – 3.39 (m, 4H, C$\underline{H_2}$OH, ring-NC$\underline{H_2}$), 3.36 – 3.34 (m, 2H, NC$\underline{H_2}$), 2.49-2.46 (m, 2H, COC$\underline{H_2}$), 1.74 – 1.69 (m, 2H, C$\underline{H_2}$CH$_2$OH), 1.64 – 1.58 (m, 6H, ring-C$\underline{H_2}$). ^{13}C{^{1}H} NMR (100 MHz, CD_3CN) δ 177.60, 58.80, 50.22, 45.16, 37.57, 31.23, 30.54, 29.16, 24.30. IR (ν/cm^{-1}): 3380 (br) (OH), 2925-2855 (C-H stretch), 1620 (C=O), 1490 (C-N), 1445-1424 (C-H).

*1-vinyl-2-pyrrolidone (**8**)*

Crystallisation: A sample of 1-vinyl-2-pyrrolidone was purchased from Sigma-Aldrich and used without further purification. Sample was loaded within a borosilicate capillary of OD 0.3 mm and mounted at 290K, and then cooled at 120 deg/h to 230K. Flash cooling (touch of liquid nitrogen) was performed when the sample was at 236 K, resulting in the formation of polycrystalline material filling the capillary. The sample was warmed to 280 K, at 120 deg/h, and melted by direct heat application (touch), noting that the crystalline material quickly re-formed. The sample was warmed to 283 K at 60 deg/h and again direct heat applied to fully melt the sample. The slow regrowth of crystalline material resulted in the formation of a good single crystal. The sample was cooled to 260 K at 60 deg/h and data collected. The sample was cooled to 150 K at 120 deg/h and a second dataset was collected. Crystal data for C_6H_9NO: M = 111.14, capillary crystallization, 0.3 x 0.3 x 0.5 mm^3, monoclinic, space group P2$_1$/c (no. 14), a = 7.6926(5) Å, b = 11.5789(5) Å, c = 7.7886(6) Å, α = 90.00^{o}, β = 118.977(10)^{o}, γ = 90.00^{o}, V = 607.10(8) Å^3, Z = 4, D_c = 1.216 g/cm^3, F_{000} = 240, T = 260K, 2θ_{max} = 52.0^{o}, 4186 reflections collected, 1186 unique (R_{int} = 0.0172). Final *GooF* = 1.048, *R1* = 0.0351, *wR2* = 0.0895, *R*

indices based on 1033 reflections with I>2σ(I) (refinement on F^2), 110 parameters, 0 restraints. Lp and absorption corrections applied, μ = 0.083 mm^{-1}.

1-(2-hydroxyethyl)-2-pyrrolidone ***(10)***

A sample of 1-(2-hydroxyethyl)-2-pyrrolidone was supplied by Ashland Inc. as a viscous yellow oil, and used without further purification. The sample was placed within a sealed vial, and submerged in a dry ice/acetone bath for 4 minutes, resulting in formation of crystalline material. A single crystal was selected and mounted upon the diffractometer. Crystal data for $C_6H_{11}NO_2$: M = 129.16, colorless block, 0.387 x 0.2127 x 0.1366 mm^3, orthorhombic, space group $Pca2_1$ (No. 29), a = 9.9709(3) Å, b = 6.6979(2) Å, c = 10.0174(3) Å, α = 90.00^o, β = 90.00^o, γ = 90.00^o, V = 669.01(4) Å^3, Z = 4, D_c = 1.282 g/cm^3, F_{000} = 280, T = 120K, 2θ_{max} = 51.9^o, 4780 reflections collected, 1301 unique (R_{int} = 0.0281). Final *GooF* = 1.056, *R1* = 0.0252, *wR2* = 0.0600, *R* indices based on 1234 reflections with I>2σ(I) (refinement on F^2), 83 parameters, 1 restraint. Lp and absorption corrections applied, μ = 0.096 mm^{-1}.

ASSOCIATED CONTENT

Supporting Information. Supporting information comprising crystallographic information in CIF format has been deposited with the Cambridge Structural Database deposition numbers CCDC 1525989-1525993. Additional IR and NMR titration data, synthetic details and crystallographic details are also available as supplementary information. This material is available free of charge via the Internet at http://pubs.acs.org. Underlying research data is

available from doi: 10.15128/r1bc386j201 in accordance with the UK research councils' open data policy.

AUTHOR INFORMATION

Corresponding Author

* Prof. Jonathan W. Steed, Durham University, Department of Chemistry, Lower Mountjoy, Stockton Road, Durham, DH1 3LE, UK, UK. Email: jon.steed@durham.ac.uk

Author Contributions

The manuscript was written through contributions of all authors. All authors have given approval to the final version of the manuscript.

Funding Sources

This work was supported by funding from the Engineering and Physical Sciences Research Council via the Doctoral Training Partnership and by Ashland Inc.

ACKNOWLEDGMENT

We thank the Engineering and Physical Sciences Research Council for funding via the Doctoral Training Partnership and Ashland Inc. for studentship funding. We also thank the Diamond Light Source for an award of instrument time on the Station I19 and the instrument scientists for support.

REFERENCES

1. Koh, C. A., *Chem. Soc. Rev.* **2002,** *31*, 157.

2. Koh, C. A.; Sloan, E. D.; Sum, A. K.; Wu, D. T., Fundamentals and Applications of Gas Hydrates. In *Annual Review of Chemical and Biomolecular Engineering, Vol 2*, Prausnitz, J. M., Ed. 2011; Vol. 2, pp 237.
3. Aman, Z. M.; Koh, C. A., *Chem. Soc. Rev.* **2016,** *45*, 1678.
4. Sloan, E. D., *Ind. Eng. Chem. Res.* **2000,** *39*, 3123.
5. Sloan Jr., E. D.; Koh, C. A., *Clathrate Hydrates of Natural Gases*. 3rd ed.; CRC Press: Boca Raton, 2007.
6. Koh, C. A.; Sum, A. K.; Sloan, E. D., *J. Appl. Phys.* **2009,** *106*, 061101.
7. Borowsky, L. BP Oil Spill Prompts Hydrate Research. http://minesmagazine.com/388/
8. Kelland, M. A., *Energy & Fuels* **2006,** *20*, 825.
9. Kelland, M. A.; Svartas, T. M.; Andersen, L. D., *J.Petroleum Sci. Eng.* **2009,** *64*, 1.
10. Perrin, A.; Musa, O. M.; Steed, J. W., *Chem. Soc. Rev.* **2013,** *42*, 1996.
11. Rojas, Y.; Lou, X., *Asia-Pac. J. Chem. Eng.* **2010,** *5*, 310.
12. Dendy Sloan, E., *J. Chem. Thermodyn.* **2003,** *35*, 41.
13. Daraboina, N.; Ripmeester, J.; Walker, V. K.; Englezos, P., *Energy & Fuels* **2011,** *25*, 4398.
14. Ohno, H.; Moudrakovski, I.; Gordienko, R.; Ripmeester, J.; Walker, V. K., *J. Phys. Chem. A* **2012,** *116*, 1337.
15. Daraboina, N.; Ripmeester, J.; Walker, V. K.; Englezos, P., *Energy & Fuels* **2011,** *25*, 4392.
16. Larsen, R.; Knight, C. A.; Sloan Jr, E. D., *Fluid Phase Equilibria* **1998,** *150–151*, 353.
17. Zhang, J. S.; Lo, C.; Couzis, A.; Somasundaran, P.; Wu, J.; Lee, J. W., *J. Phys. Chem. C* **2009,** *113*, 17418.
18. King, H. E.; Hutter, J. L.; Lin, M. Y.; Sun, T., *J. Chem. Phys.* **2000,** *112*, 2523.
19. Moon, C.; Hawtin, R. W.; Rodger, P. M., *Faraday Discuss.* **2007,** *136*, 367.
20. Anderson, B. J.; Tester, J. W.; Borghi, G. P.; Trout, B. L., *J. Am. Chem. Soc.* **2005,** *127*, 17852.
21. Carver, T. J.; Drew, M. G. B.; Rodger, P. M., *J. Chem. Soc., Faraday Trans.* **1995,** *91*, 3449.
22. Goodwin, M. J.; Musa, O. M.; Steed, J. W., *Energy & Fuels* **2015,** *29*, 4667.
23. Desiraju, G. R., *Acc. Chem. Res.* **1996,** *29*, 441.
24. Kirsh, Y. E.; Yanul, N. A.; Kalninsh, K. K., *Eur. Polym. J.* **1999,** *35*, 305.
25. Kirsh, Y. E., *Water soluble poly-n-vinylamides*. John Wiley & Sons: Chichester, 1998.
26. Maeda, Y.; Nakamura, T.; Ikeda, I., *Macromolecules* **2002,** *35*, 217.
27. O'Reilly, R.; Ieong, N. S.; Chua, P. C.; Kelland, M. A., *Chem. Eng. Sci.* **2011,** *66*, 6555.
28. Sun, S. T.; Wu, P. Y., *J. Phys. Chem. B* **2011,** *115*, 11609.
29. Spevacek, J.; Dybal, J.; Starovoytova, L.; Zhigunov, A.; Sedlakova, Z., *Soft Matter* **2012,** *8*, 6110.
30. Cohen, J. M.; Wolf, P. F.; Young, W. D., *Energy & Fuels* **1998,** *12*, 216.
31. Musa, O. M.; Cuiyue, L. Polymers having n-vinyl amide and hydroxyl moieties. WO2010117660, 2010.
32. Zhuo, J. C., *Molecules* **1999,** *4*, M117.

33. Gracias, V.; Milligan, G. L.; Aube, J., *J. Am. Chem. Soc.* **1995,** *117*, 8047.
34. Davenport, J. R.; Musa, O. M.; Paterson, M. J.; Piepenbrock, M. O. M.; Fucke, K.; Steed, J. W., *Chem. Commun.* **2011,** *47*, 9891.
35. Szaraz, I.; Forsling, W., *Polymer* **2000,** *41*, 4831.
36. Thordarson, P., *Chem. Soc. Rev.* **2011,** *40*, 1305.
37. Frassineti, C.; Ghelli, S.; Gans, P.; Sabatini, A.; Moruzzi, M. S.; Vacca, A., *Anal. Biochem.* **1995,** *231*, 374.
38. Gans, P. *HypNMR 2006*, University of Leeds: Leeds, 2006.
39. Alavi, S.; Udachin, K.; Ripmeester, J. A., *Chem.-Eur. J.* **2010,** *16*, 1017.
40. Carroll, J. J., In *Annual GPA Convention*, Calgary, Alberta, 2002.
41. Thieu, V.; Frostman, L. M. SPE International Symposium on Oilfield Chemistry, Houston, Texas, Houston, Texas, 2005.
42. Mohammadi, A. H.; Richon, D., *J. Chem. Eng. Data* **2010,** *55*, 566.
43. Mohammadi, A. H.; Richon, D., *J. Chem. Thermodyn.* **2012,** *48*, 36.
44. Kirchner, M. T.; Boese, R.; Billups, W. E.; Norman, L. R., *J. Am. Chem. Soc.* **2004,** *126*, 9407.
45. Kirchner, M. T.; Blaser, D.; Boese, R., *Chem.-Eur. J.* **2010,** *16*, 2131.
46. Perrin, A.; Myers, D.; Fucke, K.; Musa, O. M.; Steed, J. W., *Dalton Trans.* **2014,** *43*, 3153.
47. Spackman, M. A.; McKinnon, J. J., *CrystEngComm* **2002,** *4*, 378.
48. Spackman, M. A.; Jayatilaka, D., *CrystEngComm* **2009,** *11*, 19.
49. Wood, P. A.; McKinnon, J. J.; Parsons, S.; Pidcock, E.; Spackman, M. A., *CrystEngComm* **2008,** *10*, 368.
50. N-vinyl pyrrolidone. https://en.wikipedia.org/wiki/N-Vinylpyrrolidone.
51. Tishchenko, G. N.; Zhukhlistova, N. E.; Kirsh, Y. E., *Crystallogr. Rep.* **1997,** *42*, 626.
52. Corner, P. A.; Harburn, J. J.; Steed, J. W.; McCabe, J. F.; Berry, D. J., *Chem. Commun.* **2016,** *52*, 6537.
53. Dengale, S. J.; Grohganz, H.; Rades, T.; Löbmann, K., *Adv. Drug Deliv. Rev.* **2016,** *100*, 116.
54. Sheldrick, G. M., *Acta Crystallogr. Sect. C* **2015,** *71*, 3.
55. Dolomanov, O. V.; Bourhis, L. J.; Gildea, R. J.; Howard, J. A. K.; Puschmann, H., *J. Appl. Crystallogr.* **2009,** *42*, 339.
56. Barbour, L. J., *J. Supramol. Chem.* **2001,** *1*, 189.
57. Sumerlin, B. S.; Tsarevsky, N. V.; Louche, G.; Lee, R. Y.; Matyjaszewski, K., *Macromolecules* **2005,** *38*, 7540.

For Table of Contents Use Only

Hydration Behavior of Polylactam Clathrate Hydrate Inhibitors and their Small-Molecule Model Compounds

Andrea Perrin, Melissa J. Goodwin, Osama M. Musa, David J. Berry, Philip Corner, Katharina Edkins, Dmitry S. Yufit and Jonathan W. Steed*

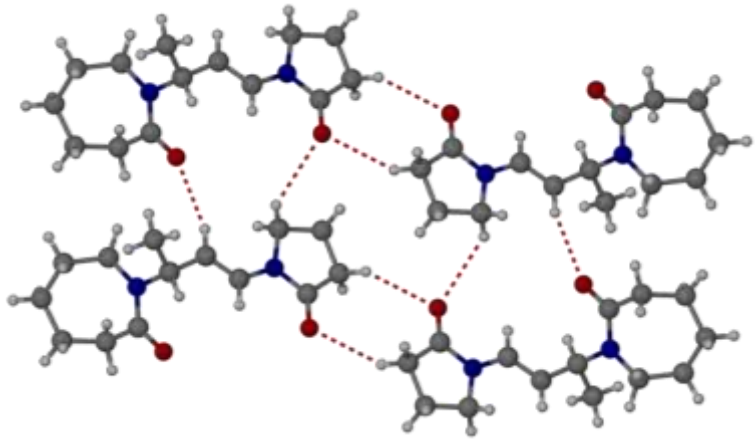

The polarity and propensity of the carbonyl groups to interact with water in a series of clathrate hydrate inhibition polylactams and their small molecule model compounds has been examined using a variety of techniques.